



Contents lists available at ScienceDirect

Applied Soft Computing

journal homepage: www.elsevier.com/locate/asoc



On decomposition methods in interactive user-preference based optimization[☆]

Jinhua Zheng^{b,a}, Guo Yu^{a,*}, Qiaofeng Zhu^c, Xiaodong Li^d, Juan Zou^a

^a School of Information Engineering, Xiangtan University, Hunan, China

^b School of Computer Science and Technology, Hengyang Normal University, Hunan, China

^c School of Mathematical and Computational Science, Xiangtan University, Hunan, China

^d School of Computer Science and IT, RMIT University, Melbourne, Australia

ARTICLE INFO

Article history:

Received 25 December 2015

Received in revised form

21 September 2016

Accepted 21 September 2016

Available online xxx

Keywords:

Optimization

Interactive multi-objective method

MOEA/D

ROI

ABSTRACT

Evolutionary multi-objective optimization (EMO) methodologies have been widely applied to find a well-distributed trade-off solutions approximating to the Pareto-optimal front in the past decades. However, integrating the user-preference into the optimization to find the region of interest (ROI) [1] or preferred Pareto-optimal solutions could be more efficient and effective for the decision maker (DM) straightforwardly. In this paper, we propose several methods by combining preference-based strategy (like the reference points) with the decomposition-based multi-objective evolutionary algorithm (MOEA/D) [2], and demonstrate how preferred sets or ROIs near the different reference points specified by the DM can be found simultaneously and interactively. The study is based on the experiments conducted on a set of test problems with objectives ranging from two to fifteen objectives. Experiments have proved that the proposed approaches are more efficient and effective especially on many-objective problems to provide a set of solutions to the DM's preference, so that a better and a more reliable decision can be made.

© 2016 Elsevier B.V. All rights reserved.

1. Introduction

In real life, most optimization problems involving multiple conflicting criteria, so-called multi-objective optimization problems (MOPs), are hard to solve by traditional optimization methods, but the multiple criteria decision making (MCDM) [3] and the evolutionary multi-objective optimization (EMO) methodologies [4] have been demonstrated that they can find a set of well-distributed trade-off solutions [4,5] approximating the Pareto-optimal front. In particular, EMO techniques have been successfully applied to some real-world applications like optimal control [6], data mining [7], robot path planning [8], job scheduling [9], etc.

Nevertheless, the multi-objective evolutionary algorithms (MOEAs) experienced many difficulties when dealing with many-objective optimization problems. The many-objective evolutionary problems refer to the optimization problems with more than 3 objectives [10]. There are four representative sorts of methods or

techniques proposed to solve many-objective problems. The first category is based on improved Pareto-dominance relationship, like CDAS [11], ϵ -MOEA [12,13], and fuzzy dominance [14,15], etc. The second class is based on indicators or metrics, like ϵ indicator and HV indicator based IBEA [16], HV indicator based SMS-EMOA [17] and HypE [18], etc. The third class is based on aggregation and ranking, like MOEA/D [2], MSOPS [19], NAGA-III [20], AR [21], etc. The fourth category is based on estimation, like DMO [22], SDE [23], etc.

Although the proposed methods and techniques have been demonstrated to deal with many-objective problems effectively to some extent, recent studies [24,25] suggest that EMO algorithms face many challenges in solving MOPs with large numbers of objectives. First, when the number of objectives are more than 3, the visualization of the objective space is challenging, and EMO algorithms have significant difficulties in finding the entire Pareto-optimal front. Apart from searching a much larger objective space, the optimization algorithm needs a much larger population in order to find solutions to cover a much larger Pareto-optimal frontier surface. Moreover, how many solutions should be included to achieve an even spread of Pareto-optimal solutions remains questionable. However, we can tackle this problem from a different angle: EMO algorithms could put more computational effort on searching the region of interest (ROI) [1] rather than the entire Pareto-optimal frontier. This point of view has practical meaning and allows the

[☆] Fully documented templates are available in the elsarticle package on CTAN.

* Corresponding author.

E-mail addresses: jhzhang@xtu.edu.cn (J. Zheng), yuguo0801@126.com (G. Yu), lursonkj@gmail.com (Q. Zhu), xiaodong.li@rmit.edu.au (X. Li), zoujuan@xtu.edu.cn (J. Zou).

decision maker (DM) to focus only around the ROIs rather than the entire Pareto-optimal frontier. Furthermore, in MCDM literature, it is generally considered a good practice to involve the DM into the optimization process by providing his/her preference information. This “human-in-the-loop” approach can help the optimization algorithm to adapt its search process in order to find the most appropriate solutions for the decision makers.

Depending on when the DM intervenes the search process, i.e., before, during or after the search process, the EMO or MCDM approaches can be classified into three categories: a priori, interactive and a posteriori methods.

For a priori approach, the DM needs to provide the preference information before the optimization process starts. This can be achieved by either specifying reference points, a mathematic model of the preference information, weighting information, etc. However, in reality, this is rarely the case.

For the interactive approach, the DM can make adjustment to the search preferences, based on the feedback received during the search. The interactive approach has many advantages. First, it could assist the DM in learning about the problems and guide the optimization process towards the ROIs and away from the uninteresting areas, resulting in substantial saving on computational resources. Second, it could facilitate finding multiple ROIs in response to differing preferences simultaneously. Third, it could find the ROIs for the DM in a single run based on the interactive preference-based optimization rather than repeatedly start the optimization to find the trade-off solutions.

With a posteriori methods, the DM only makes use of the preference information after the optimization process ends. This is perhaps the most common form of EMO methods in the literature. However, when dealing with many-objective problems, this approach is less effective since the computational burden for finding solutions across the Pareto-frontier increases exponentially with the increasing number of the objectives. It is also less efficient considering the vastness of the search space. It would make far better sense if the algorithm concentrates only on the ROI of the Pareto-front that is expressed by the DM.

Among these three methods, the a priori and interactive methods are particularly appealing, and have been adopted by several algorithms hybridizing EMO and MCDM methods. Branke [26] and Deb [27] proposed a guided multi-objective evolutionary algorithm (G-MOEA) based on modified dominance relationship upon the DM's preference information. Deb et al. integrated the reference point [28] and reference direction [29] into the interactive EMO algorithm respectively. Besides, Thiele et al. [30] suggested reference point based EMO procedures to find a set of points close to the specified multiple reference points. Molina [31] and Ben [32] proposed g -dominance relationship and r -dominance relationship respectively, which both modified the Pareto-dominance relationship with the reference point, but the former focuses on one reference point and is based on a priori; the later is one sort of multiple reference points based interactive method.

The decomposition-based multi-objective evolutionary algorithm (MOEA/D) [2] tries to decompose the MOP into a set of single-objective problems by introducing a group of uniform weight vectors. Thus, MOEA/D [2] is one sort of MCDM approaches that can be applied to the preference-based model. Gong et al. [33] proposed an interactive MOEA/D [2] with user-preference; during the optimization process, the weights of selected solutions will be used to guide the search to find the preferred region. Mohammadi et al. [34] also gives the reference points based MOEA/D. On the bases of light beam search [35] and the decomposition-based MOEA/D [2], Yu et al. [36] proposed a MOEA to decompose or transfer the preference information of the reference point specified by the DM into a number of scalar optimization sub-problems and deal with them simultaneously.

However, on the basis of formal work [33,34,36], no attempts have been made to use the preference information in the many objective context. Both papers [33,36] are designed only to satisfy single preference based model. Therefore, this paper attempts to develop a preference-based interactive model extending to the framework of MOEA/D, to search for the ROIs simultaneously in terms of different preference information. We will propose and analyze several methods how to apply the preference information into the frame. Thus, this paper tries to provide the decision-maker with a set of Pareto-optimal solutions to the DM's preference so that a better and a more reliable decision can be made.

The remainder of the paper is organized as follows. In Section 2, we introduce the multi-objective problem and some related definitions. In Section 3, some related work including the achievement scalarizing function [38], interactive method [28,30,29], and the MOEA/D [2], will be presented. Section 4 describes the proposed model, which essentially combines the MOEA/D framework with an interactive method using multiple reference points. The experimental results are presented and analyzed in Section 5. Finally, Section 6 concludes the paper.

2. Multi-objective optimization

A multi-objective problem (MOP) can be formulated mathematically in the following form:

$$\begin{aligned} \text{minimize : } & F(x) = (f_1(x), \dots, f_m(x))^T \\ \text{subject to : } & x \in \Omega \end{aligned} \quad (1)$$

where x denotes a solution vector in the decision space Ω . $F: \Omega \rightarrow R^m$ consists of m real-valued objective functions. R^m is called the objective space.

If $x \in \Omega$, all the objectives are continuous and Ω is described by $\Omega = \{x \in R^n | h_j(x) \leq 0, j = 1, \dots, k\}$, where h_j are continuous functions. We call problem (1) a continuous MOP.

The mathematically equivalent solutions in problem (1) are denoted as Pareto-optimal solutions. The related definitions are as follows:

Definition 1. In problem (1), a vector $x \in \Omega$, is said to Pareto dominate another vector $y \in \Omega$, which denotes as $x \prec y$, if $\forall i \in \{1, 2, \dots, m\}$, s. t. $f_i(x) \leq f_i(y)$ and $\exists j \in \{1, 2, \dots, m\}$, s. t. $f_j(x) < f_j(y)$.

Definition 2. In problem (1), a vector $v \in \Omega$, is nondominated if $\nexists w \in \Omega$, s. t. $f_i(v) \leq f_i(w)$, for all $i \in \{1, 2, \dots, m\}$.

Definition 3. In problem (1), a vector $\iota \in \Omega$, is weakly nondominated if $\nexists k \in \Omega$, s. t. $f_i(\iota) < f_i(k)$, for all $i \in \{1, 2, \dots, m\}$.

Definition 4. In problem (1), the set $X \subset \Omega$ of all the nondominated solutions is called the nondominated or Pareto-optimal set (PS). The Pareto-optimal front (PF) is the image of PS in the objective space.

Definition 5. The Pareto-optimal solutions in the region of interest (ROI) [1] are preferred solutions according to the decision maker (DM). As shown in Fig. 2, the ROI is one small region on the PF close to the reference point, and the solutions in the ROI are preferred solutions.

In Fig. 1, in objective space, solution A dominates solution B since $f_1(A) < f_1(B)$ and $f_2(A) < f_2(B)$.

3. Related works

3.1. Preference model

For problem (1), in the objective space, there are two main regions: the feasible region and infeasible region as shown in Fig. 1. The feasible region is above the PF. All objectives of the solution in

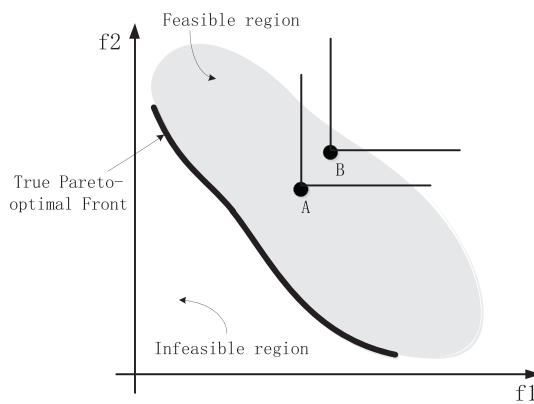


Fig. 1. Illustration of the objective space, dominance relationship, and PF.

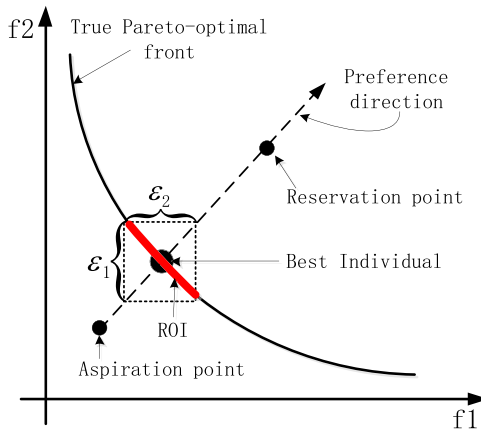


Fig. 2. Illustration of the preference relation model.

the feasible region can be reached. These solutions are denoted as feasible solutions. Similarly, the infeasible region is below the PF, and the solutions in the infeasible region are denoted as infeasible solutions.

Considering the perspective of the DMs, they have different interests in varying objectives. Thereby, the MOEAs need not sort all of the Pareto solutions approximating the PF but only the region of interest (ROI) based on the DM's preference or demand. In terms of DM's preference information, Jaszkiewicz et al. gave a general preference model of the light beam search (LBS) methodology and application [35]. In this model, the DM should give the aspiration point, reservation point, indifference threshold, preference threshold and veto threshold.

In order to simplify the former model, Deb et al. gave a simplification model [37] as shown in Fig. 2. The preference direction is essentially that of the vector from the aspiration point to the reservation point. The intersection is the best solution or individual. The region around the best point and highlighted with a red is the region of interest (ROI) [1]. This model allows the DM to specify his/her desired region through a reservation point (reference point). In this model, it integrates the preference information into the optimization to guide a more focused searching, so that a multitude of computational resources can be saved. Thus, the model is widely used in the preference based optimization [4,5,31,32].

3.2. Achievement scalarizing function (ASF)

Dozens of MCDM methods often applied the achievement scalarizing function (ASF) which was first proposed by Wierzbicki [38]. The ASF is to project any specified feasible or infeasible point

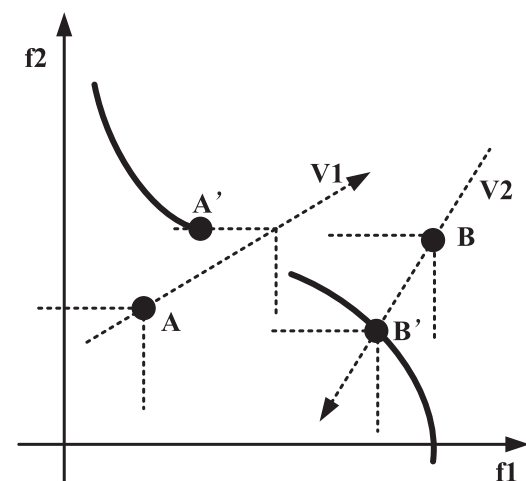


Fig. 3. Illustration of achievement scalarizing function.

$g \in R^m$ onto the set of Pareto-optimal solutions [39]. The point g is called a reference point, and its components' values are specified by the DM and called aspiration levels. More information about ASF is also presented in [3].

A typical form of ASF to be minimized is:

$$\begin{aligned} \text{minimize : } & \text{ASF}_g(F(x)) = \max_{i=1}^m [\omega_i(f_i(x) - g_i)] \\ \text{subject to : } & x \in R^n \end{aligned} \quad (2)$$

where $F(x)$ is one obtained solution in the objective space to the problem defined in Eq. (1); g is the given reference point; $\omega_i > 0$ for all $i = \{1, 2, \dots, m\}$ is the i th component of a chosen weight vector $\vec{\omega}$. The weight vector is used for scalarizing the objectives. $f_i(x)$ is the i th objective of solution $F(x)$.

In Fig. 3, v_1 and v_2 are the directions of aggregation. The starting points of v_1 and v_2 are the reference points A and B , and the directions of v_1 and v_2 are based on different given weight vectors $\vec{\omega}$. The thick solid lines are the Pareto-optimal front, and the dotted lines represent the directions of v_1 and v_2 respectively. Point A' and point B' are the corresponding Pareto-optimal solutions obtained by ASF. Thus, it is obvious from the figure that ASF could provide with the best preferred solution in the DM's ROIs.

3.3. Interactive preference method

The preference-based EMO algorithms aim to find the Pareto-optimal solutions in the ROI. For example, Wierzbicki [38] suggested a reference point based approach. By means of ASF, the approach could achieve a weakly Pareto-optimal solution which is closest to the specified reference point of aspiration level based on achievement scalarizing problem. In other words, ASF can be applied in the interactive-preference model.

To build an interactive MOEA/D model, following properties will be considered:

- The system should generate Pareto-optimal or weakly Pareto-optimal solutions;
- The system needs to provide the best candidate solutions or alternative preferred solutions for the DM;
- The system could help the DM to understand the global information of the Pareto-optimal set;
- The system needs to be efficient and effective;
- The communication system is not complicated for the DM.

In literature [28–31,33], the interactive method can be generally described in the following steps:

- Step 1. Initialization: Without the guidance of preference information, find a rough approximating Pareto-optimal solution set by using an EMO algorithm, and select solutions in the set to characterize the approximation and present them to the DM.
- Step 2. Preference information: In accordance with the alternative solutions, DM specifies his/her preference information (such as reference point, preference direction, ROIs etc.).
- Step 3. Local approximation: On the basis of the preference information, EMO algorithm tries to search for the local approximating Pareto-optimal solution set. For example, the EMO algorithm tries to find the Pareto-optimal solutions in the ROIs.
- Step 4. Projection of the preference information: By means of the solution set obtained in Step 3, display the Pareto-optimal solutions to the DM and find the best desired solution for the DM. For example, among the alternative solution set, use the ASF to find the best solution closest to the reference point.
- Step 5. Termination: If the DM is satisfied with the providing best solution, then stop the searching; otherwise, go to Step 2 and continue the program.

3.4. Decomposition-based algorithm (MOEA/D)

The ideal of decomposition-based multi-objective evolutionary algorithm (MOEA/D) [2] is to decompose a multi-objective optimization problem into a set of scalar optimization subproblems or single-objective optimization problems and to optimize them simultaneously. Each subproblem is optimized by incorporating the information from its neighboring subproblems. MOEA/D needs a group of uniform spread of weight vectors $\lambda^1, \lambda^2, \dots, \lambda^N$, and each $\lambda^j = (\lambda_1^j, \lambda_2^j, \dots, \lambda_m^j)$ satisfies $\sum_{k=1}^m \lambda_k^j = 1$ and $\forall \lambda_k^j \geq 0$, where m is the number of objectives, and N is the size of population.

There are several aggregation methods or scalar functions including the weighted sum approach [3], Tchebycheff approach [3], and penalty-based boundary intersection (PBI) approach [2] to convert the MOP (1) into a number of subproblems.

3.4.1. Weighted sum approach

The weighted sum approach is a well-known aggregation method and the j th minimization sub-problem is as follows.

$$\text{minimize : } g^{ws}(\vec{x} \mid \lambda^j) = \sum_{i=1}^m \lambda_i^j f_i(\vec{x}) \quad (3)$$

subject to : $\vec{x} \in \Omega$

where $i \in \{1, \dots, m\}$, and m is the number of objectives.

3.4.2. Tchebycheff approach

The j th scalar optimization problem in this approach adopts the following form.

$$\text{minimize : } g^{tche}(\vec{x} \mid \lambda^j, z) = \max_{1 \leq i \leq m} \lambda_i^j |f_i(\vec{x}) - z_i| \quad (4)$$

subject to : $\vec{x} \in \Omega$

where z is the ideal point and defined as $z = (z_1, \dots, z_m) = (\min_{i=1}^N f_i^i, \dots, \min_{i=1}^N f_i^i)$.

3.4.3. Penalty-based boundary intersection (PBI)

In this approach, the j th scalar optimization problem of PBI is the following:

$$\text{minimize : } g^{pbi}(\vec{x} \mid \lambda^j, z) = d_1 + \theta d_2 \quad (5)$$

subject to : $\vec{x} \in \Omega$

where

$$d_1 = \frac{\|(z - F(\vec{x}))^\top \lambda^j\|}{\|\lambda^j\|},$$

$$d_2 = \|F(\vec{x}) - (z - d_1 \lambda^j)\|,$$

z is the ideal point and $\theta > 0$ is a user-specified penalty parameter.

3.4.4. The framework of MOEA/D

The main framework of MOEA/D is presented in [Algorithm 1](#). Lines 1–5 are the initiation stage. NS_i in line 2 is the neighbor index set and consists of the indexes of T closest weight vectors of λ^i ; line 3 is to initialize the population $P = \{x^1, \dots, x^N\}$; line 4 is to compute the fitness of each individual; in line 5, it is to initialize the ideal point $z = (\min_{i=1}^N f_i^i, \dots, \min_{i=1}^N f_i^i)$ in the current population P . Line 6–19 is the update stage; in the framework, $g^{te}(x' \mid \lambda^j, z)$ is one of the following 3 methods: Tchebycheff, Weighted Sum, or PBI; in line 8, randomly select two indexes from NS_i , then generate a new solution x from x^k and x^l by crossover operator, then line 9 updates the solution x by a mutation operation. Lines 11–15 show that the new solution x' will update every neighbor subproblem if its fitness $g^{te}(x' \mid \lambda^j, z)$ is smaller than that of the solution y^j , where y^j is the elite solution in the j th closest subproblem. When a new solution is generated, then update the ideal point z and elite population EP .

Algorithm 1. The framework of MOEA/D

Input: MOP: the multi-objective optimization problem; N : the size of population; weight vectors: $\lambda^1, \dots, \lambda^N$; T : the size of the neighborhood of each weight vector; \mathcal{T} : Terminate Condition.

Output: Elite Population: EP

```

1:   EP = ∅
2:   NSi = {i1, ..., iT}, i = 1, ..., N.
3:   RandomInitPopulation(P)
4:   Evaluation(P)
5:   Init(z)
6:   while  $\neg \mathcal{T}$  do
7:     for each  $i = 1, \dots, N$  do
8:       x = Crossover(k, l, NSi)
9:       x' = Mutation(x)
10:      Evaluation(x')
11:      for each j ∈ NSi do
12:        if  $g^{te}(x' \mid \lambda^j, z) \leq g^{te}(y^j \mid \lambda^j, z)$  then
13:          yj = x'
14:        end if
15:      end for
16:      Update(EP)
17:      Update(z)
18:    end for
19:  end while

```

From the framework of MOEA/D, it is obvious that the diversity of the final obtained solutions is determined by the uniformity of the weight vectors, because MOEA/D decomposes the MOPs into a group of single-objective optimization problems by means of a set of uniform weight vectors.

4. Proposed approaches

In this section, we will firstly introduce three approaches on how to combine the MOEA/D with the preference information respectively. Then some key issues are analyzed and solved in the next subsection. Lastly, the main framework of the interactive MOEA/D with multiple preference information will be presented.

4.1. The proposed preference models

Recently, the framework of MOEA/D [2] has been used in the user-preference information based model. For example, the iMOEA/D [33] incorporates the preference information (weight

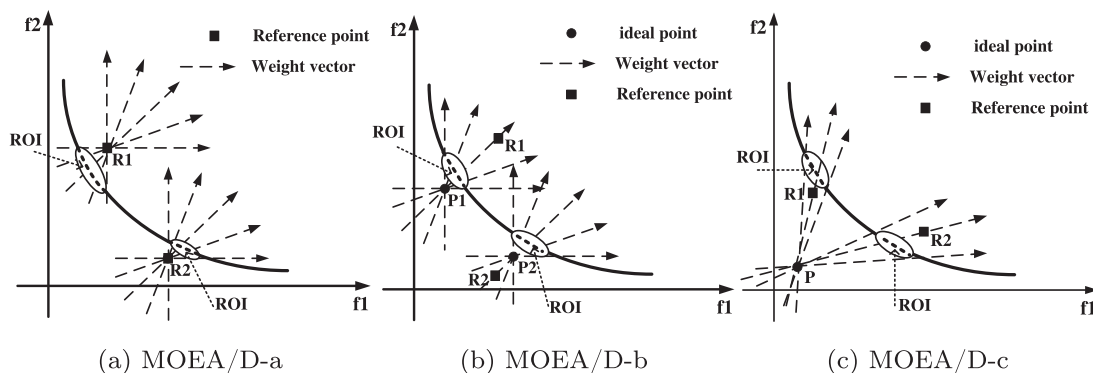


Fig. 4. Illustration of the models of how to incorporate the preference information (the reference point) into MOEA/D.

vector) into MOEA/D to find the ROI. Reference point based MOEA/D [34,36] applies the information of reference points to guide the optimization process to search for the ROIs. However, [33,34] did not consider many-objective problems, and none of them have taken both of multiple preference information¹ and interactive model into consideration simultaneously. Actually, more preference information considered during the interactive process could assist the DM in learning more about the problems especially on many-objective problems; and it could find interesting solutions in multiple ROIs interacting with the DM's preferences simultaneously; thus it could provide more useful information or alternative solutions to the DM. Besides, there is another issue to be noted that the locations of the reference points (in the feasible region or in the infeasible region) will impact the performance of the procedure.

Given the above consideration, we try to find the general framework of MOEA/D based on user-preferences to handle the aforementioned issues. Looking inside of MOEA/D, we find that the key issue is how to adjust the weight vectors or neighboring weight vectors in response to the preference information. Taking the reference points as the preference information for example, this paper proposes three methods on how to incorporate the preference information (reference points) into MOEA/D as shown in Fig. 4.

In Fig. 4, the three sub-plots all have two different reference points (the one is set in feasible objective space, and the other one is in infeasible objective space). The key difference amongst them is the relationship between weight vectors and reference points.

- The weight vectors in sub-plot 4(a) are only related to the reference points. This method is similar to the g-dominance relationship [31] but could obtain different ROIs simultaneously by applying multiple reference points to guide the optimization to find the ROIs. Besides, the approach could adjust the weight vectors to modify the range of ROIs. The approach denoted as MOEA/D-a in sub-plot 4(a) only cares about the solutions adjacent to the weights, and optimizes the subproblems simultaneously to obtain the ROIs.
 - Sub-plot 4(b) is similar to the first one, but the advantage of this approach (denoted as MOEA/D-b) is that it connects the ideal points and the corresponding reference points to determine the center weight vectors so as to determine the searching directions.

in the objective space. Also, MOEA/D-b can adjust the range of ROIs as well.

- Different with Sub-plot 4(b), MOEA/D-c in Sub-plot 4(c) only uses the ideal point of the entire population and different reference points to determine the center weight vectors. The searching objective space and the range of ROIs can be adjusted by varying the weight vectors as well.

4.2. Key issues in the models

In the three models, there are two main issues to address. First, it is to pinpoint the relationship between the weight vectors and scalar functions. Second, it is how to get the ideal points in sub-populations.

4.2.1. The weight vectors and scalar functions

As shown in Fig. 4, about the three scalar functions introduced in Section 3.4, both the Tchebycheff and PBI approach can be used in the model of MOEA/D-b and MOEA/D-c because the weighted sum approach does not require the ideal point.

Notably, for MOEA/D-a, the ASF illustrated in Section 3.2 can be applied in the framework. Comparing the ASF with the Tchebycheff approach, we could find the similarity between them, i.e., both methods aim to find the point near the reference point and ideal point. However, if we replace the ideal point in the Tchebycheff approach with the reference point directly, MOEA/D-a would be ineffective when the reference point is in the feasible region. The main reason is that the offsprings, located in the position between the reference point and PF, cannot be preserved in terms of the scalar function. On the contrary, ASF is effective as the solutions will approximate the Pareto-optimal front as closely as possible by comparing their ASFs in the subproblems.

The original iterative weight approach [36] generates the weight vectors in the objective space by using $f_1 + \dots + f_m = 1$ directly, however, in most cases, $f_1 + \dots + f_m = 1$ is unknown. Besides, the approach optimistically uses the light beam from the original to the reference point to determine the center weight vector. In fact, the ideal points would be more practical instead of the original point. Hence, here we introduce the modified iterative weight approach which will be used in the following experiments in Section 5.

Fig. 5 presents the mapping relationship in the two-dimensional model of the improved iterative weight approach. The details are as follows.

¹ For example, multiple reference points are specified to guide the optimization process to obtain solutions in different ROIs.

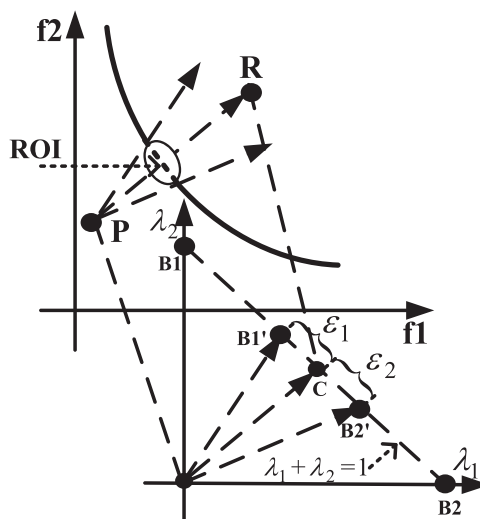


Fig. 5. Illustration of the two-dimensional model of improved iterative weight approach.

(shown in Fig. 5) in the weight vector space. The i th component of λ_0 is the following:

$$\lambda_0^i = \frac{|R_i - P_i|}{\sum_{i=1}^m |R_i - P_i|}$$

Step 2: Compute the outer boundary point set $O = \{(1, 0, \dots, 0), (0, 1, \dots, 0), \dots, (0, 0, \dots, 1)\}$. For example, the outer boundary point set is $O = \{B_1, B_2\}$ in Fig. 5.

Step 3: Compute the inner boundary point set I by means of $\varepsilon = (\varepsilon_1, \dots, \varepsilon_m)$ which controls the range of ROI, and $\varepsilon_i \geq 0 \wedge \varepsilon_i \leq 1, i = \{1, \dots, m\}$. The i th point B'_i in I can be obtained by $\vec{CB}'_i = \varepsilon_i \cdot \vec{CB}_i$, where B_i is the i th point in O . Then add the set I into the set of weight vectors ϖ like $\varpi = \varpi \cup I$. For example, the inner boundary point set $I = \{B'_1, B'_2\}$ in Fig. 5 can be obtained by the following expression.

$$\begin{cases} \vec{CB}'_1 = \varepsilon_1 \cdot \vec{CB}_1 \\ \vec{CB}'_2 = \varepsilon_2 \cdot \vec{CB}_2 \end{cases}$$

Step 4: Obtain the midpoint of set M through computing the intermediate points of any two points in the point set ϖ .

Step 5: Obtain the other midpoint of set M' through computing all of the intermediate points between every point in set M and every point in the set ϖ .

Step 6: $\varpi = \varpi \cup M, M = M'$.

Step 7: Iterate the steps 4, 5, 6 till $|\varpi|$ equals the required number of weight vectors.

Fig. 6 is the result of 3-objective weight vectors obtained by iterative weight approach with $\varepsilon = (1.0, 1.0, 1.0)$, reference point $R = (0.5, 0.5, 0.5)$, and ideal point $p = (0.01, 0.01, 0.01)$.

4.2.2. Ideal points in sub-populations

The ideal point is the point whose objective values are the smallest in the population. It can be denoted as $z = (z_1, \dots, z_m) = (\min_{i=1}^N f_1^i, \dots, \min_{i=1}^N f_m^i)$, where N is the size of population.

As for MOEA/D-c, it uses the ideal point of the whole population to determine the direction of the weight vector. Thus the original ideal point is $z = (z_1, \dots, z_m) = (\min_{i=1}^N f_1^i, \dots, \min_{i=1}^N f_m^i)$, where N is the size of whole population.

As for MOEA/D-b, it adopts multiple sub-populations in the optimization. Each reference point corresponds to a sub-population. The simplest way to get the sub-population is to use the Euclidean distance to search for the solutions in the whole population close to the reference point. Thus, in MOEA/D-b, the ideal point in each sub-population is denoted as $z = (z_1, \dots, z_m) = (\min_{i=1}^S f_1^i, \dots, \min_{i=1}^S f_m^i)$, where S is the size of sub-population.

4.3. The framework of interactive preference-based MOEA/D

Algorithm 2 illustrates the main framework of the interactive preference based MOEA/D. It applies the basic framework of MOEA/D presented in Section 3.4 and adds some mechanisms to combine the preference information into the framework. Here, we take the reference point as the preference information for example. Of course, other methods for specifying preference information can be also applied here.

Algorithm 2. The framework of interactive preference-based MOEA/D

Input: MOP: the multi-objective optimization problem; ℓ : the number of reference points; N : the size of population P ; ϵ : the range of ROI; T : the size of the neighborhood of each weight vector; \mathcal{T} : Terminate Condition.

Output: Elite Population: EP

```

1:   EP = ∅
2:   RandomInitPopulation(P)
3:   for each  $m = 1, \dots, \ell$  do
4:     DividePop(SubPop)
5:     Evaluation(SubPop)
6:     Init(z)
7:     InitWeight( $\lambda$ ,  $\epsilon$ )
8:     Init(NS)
9:   end for
10:  while  $\neg \mathcal{T}$  do
11:    EvaluationASF(EP)
12:    Interaction(PreferenceInformation)
13:    for each SubPop do
14:      for each  $i = 1, \dots, |\text{SubPop}|$  do
15:         $x = \text{Crossover}(k, l, NS_i)$ 
16:         $x' = \text{Mutation}(x)$ 
17:        Evaluation(x')
18:        for each  $j \in NS_i$  do
19:          if  $g^{te}(x' | \lambda^j, z) \leq g^{te}(y^j | \lambda^j, z)$  then
20:             $y^j = x'$ 
21:          end if
22:        end for
23:        Update(EP)
24:        Update(z)
25:        Update( $\lambda$ ,  $\epsilon$ )
26:      end for
27:    end for
28:  end while
```

The interactive preference-based MOEA/D decompose the MOP into a set of subproblems with a group of uniform weight vectors, then optimizes the subproblems simultaneously. During the optimization, the approach, on the basis of the preference information specified by the DM, tries to adjust its weight vectors and subproblems and searches for the solutions in the ROIs for the DM. In the framework, line 11 is to evaluate the provided solutions by means of the ASF functions, and line 12 is to integrate the DM's preference information (like the reference points, and ϵ the range of ROI) into the optimization in terms of the evaluation. According to the specified preference information, lines 13–27 optimize the sub-populations simultaneously to search for the desired Pareto-optimal solutions or ROIs. When the DM specifies different preference information, or the ideal points are changed, the weight vectors will be updated in line 25.

In the following experiments, in the line 12, the preference information is specified with the reference points and a parameter

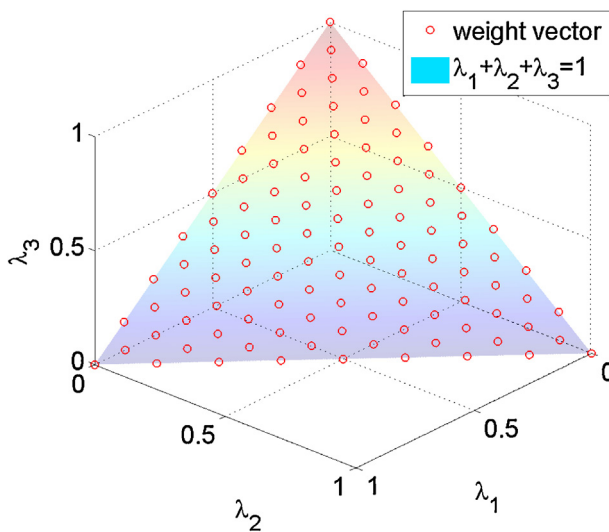


Fig. 6. The 3-objective weight vectors obtained by improved iterative weight approach with reference point $R=(0.5, 0.5, 0.5)$ and $\epsilon=(1.0, 1.0, 1.0)$.

$\epsilon \in [0, 1]$ which controls the size of ROI. The details of ϵ is illustrated in Section 4.2.1.

5. Experiments

In this section, experiments will be conducted to demonstrate the feasibility of these new approaches which could find the solutions in different ROIs according to the varying preference information of the DM. Besides, it also tries to prove that the proposed approaches could deal with many-objective problems.

All of the experiments are conducted 30 times independently. About the three proposed approaches used in the following experiments, MOEA/D-b and MOEA/D-c apply the PBI approach with the $\theta=5$ and $T=10$ (default values used in MOEA/D), additionally, the MOEA/D-a adopts ASF as its aggregation approach in the optimization. The 2-objective ZDT1, ZDT2 problems [40] and 3-objective DTLZ1, DTLZ2 problems [41] are selected as the test instances and will be discussed respectively. After that, on dealing with many-objective problems, the many-objective DTLZ2 with 10 objectives and 15 objectives will be selected. All the simulations were run on a personal computer with Intel(R) Core(TM) i5 CPU @2.67GHz and 2G RAM.

5.1. Parameter settings

About the experiment, the population size N is set to be 100 for 2-objective test instances, and 300 for 3-objective test instances, 500 for many-objective instances respectively. The sub-population size is N/ℓ , and ℓ is the number of reference points. The algorithm will stop after 500 generations and the results are based on 30 independent runs. Besides, in all simulations, we use the differential evolution crossover operator with the $CR=1.0$ and $F=0.5$, and polynomial mutation operator with an index 20 [4].

Following the practice in the interactive model [33], there are three interactions during the optimization process. In this paper, the DM will interfere the optimization process after each 100 generations. Before the interaction, algorithms should run in advance to obtain the alternative solutions for the DM to specify his/her preference. The preparation stage ($H=0$) will cost 200 generations. After that, it is the first interaction stage ($H=1$), the DM could specify his/her preference information. In the second interaction stage ($H=2$) after 300 generations, the DM could adjust his/her preference information. About interaction stage three ($H=3$) after 400

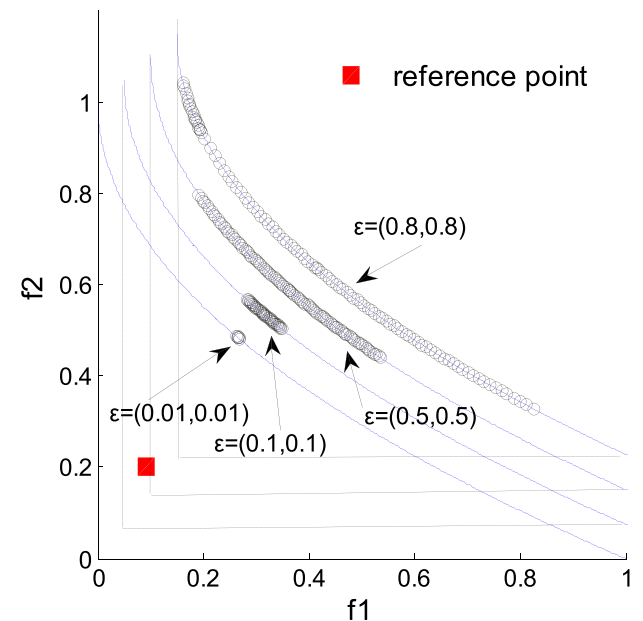


Fig. 7. Effect of different values of ϵ in obtaining varying ranges of ROIs on ZDT1.

generations, slight modification of the preference information will be presented by the DM to guide the searching process to the desired ROIs.

5.2. Results on 2-objective MOPs

In this section, we consider the 30-variable ZDT1 and ZDT2 problems, and will present them as follows.

ZDT1 has a concave Pareto-optimal frontier and its equation $F=(f_1(x), f_2(x))$ is as follows:

$$\begin{cases} f_1(x) = x_1, \\ f_2(x) = g(1 - \sqrt{f_1/g}) \end{cases} \quad (6)$$

where $g(x) = 1 + 9\sum_{i=2}^m x_i/(m-1)$, $m=30$, $0 \leq x_i \leq 1$, $i=\{1, \dots, n\}$. Here, $n=30$ in the experiment.

ZDT2 has a non-convex Pareto-optimal frontier. It is illustrated as follows:

$$\begin{cases} f_1(x) = x_1, \\ f_2(x) = g(1 - (f_1/g)^2) \end{cases} \quad (7)$$

where $g(x) = 1 + 9\sum_{i=2}^m x_i/(m-1)$, $m=30$, $0 \leq x_i \leq 1$, $i=\{1, \dots, n\}$. Here, $n=30$ is set in the experiment.

5.2.1. Ability to control the range of ROI

In the preference-based model, how to adjust the model to satisfy the user-preference is one of the essential abilities.

Fig. 7 shows the effect of varying values of ϵ in obtaining different ranges of ROIs on ZDT1 obtained by MOEA/D-a with the reference point $(0.1, 0.2)$. With the increase of the value of ϵ , the range of the ROIs enlarges correspondingly. Thus, if the DM is willing to obtain a large neighborhood of solutions near the ROI, a large value of ϵ would be chosen.

Thus, from the plot, we can find that the proposed approaches have the ability to control the extent of ROIs.

5.2.2. Results on ZDT1 and ZDT2

To test the ability of the proposed approaches to handle 2-objective MOPs, Figs. 8 and 9 show the results obtained by three different approaches after each interaction process.

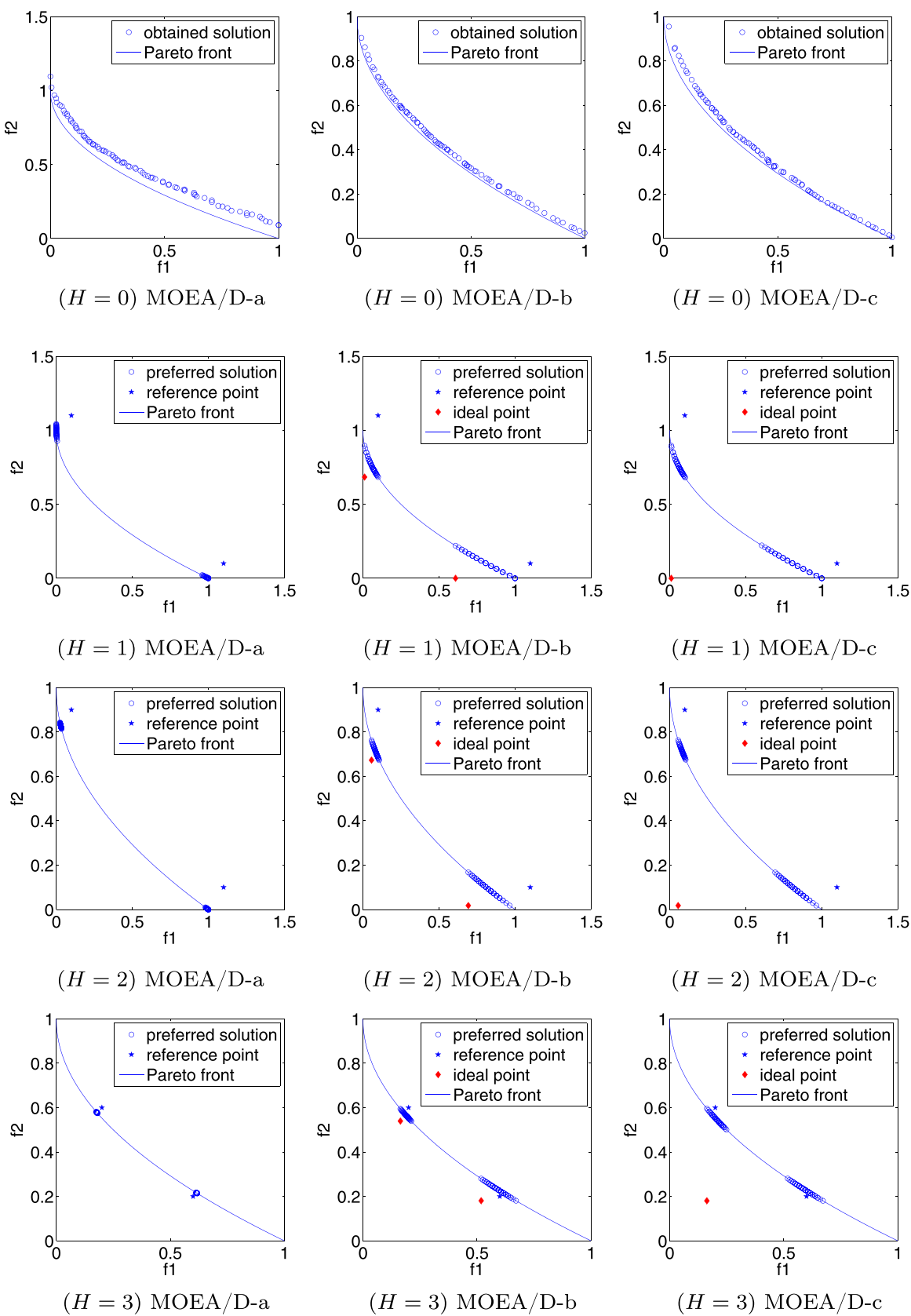


Fig. 8. Results on ZDT1 obtained MOEA/D-a, MOEA/D-b and MOEA/D-c in different stages.

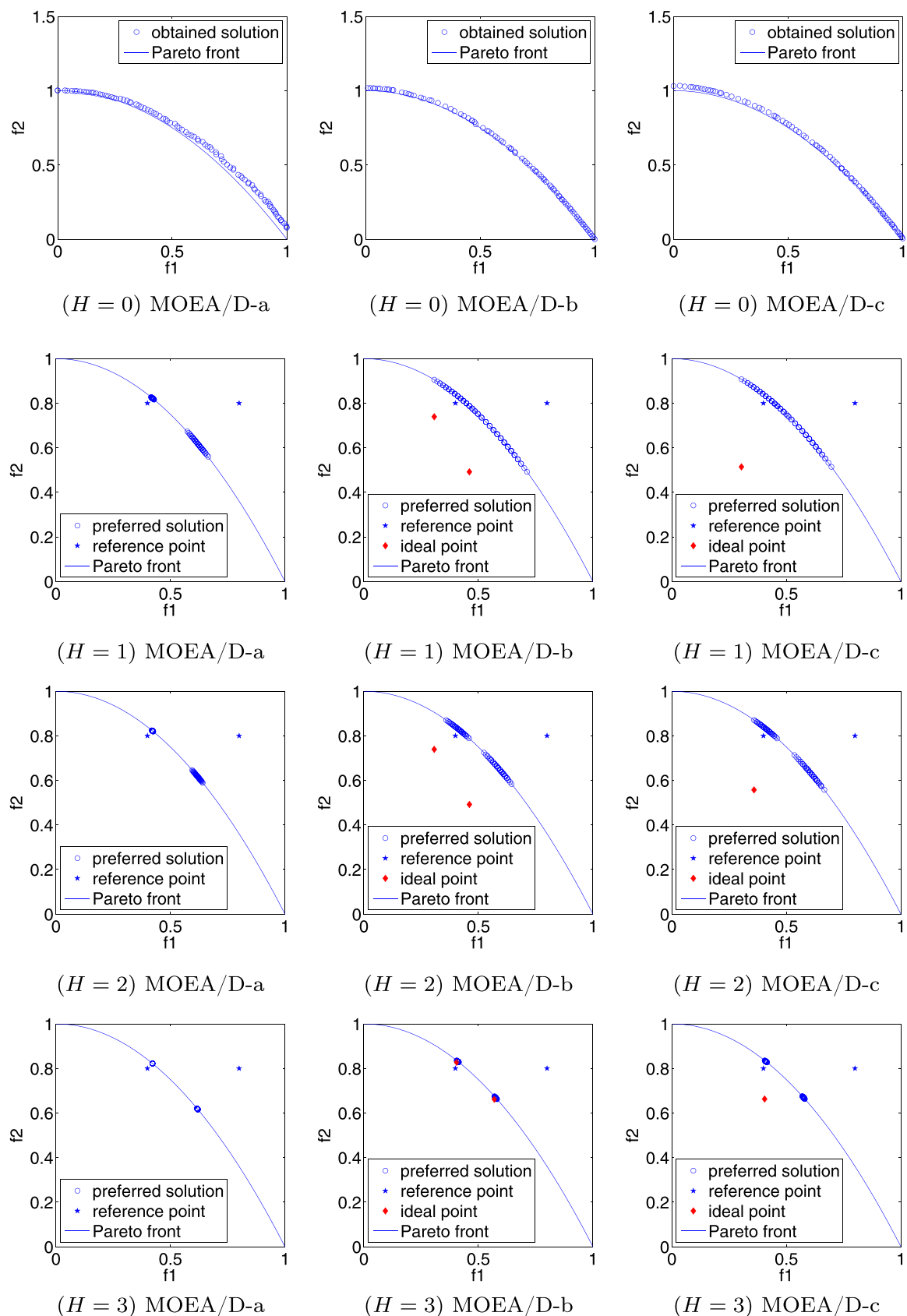


Fig. 9. Results on ZDT2 obtained MOEA/D-a, MOEA/D-b and MOEA/D-c in different stages.

The first row, in Figs. 8 and 9, presents the results of the preparation stage ($H=0$) on ZDT1 and ZDT2 respectively. The entire population almost approaches to the Pareto-optimal front.

After the preparation stage with 200 generations, the DM interferes the optimization process, and specifies some reference points like $(1.1, 0.1)$, $(0.1, 1.1)$ and $\epsilon=(0.2, 0.2)$ to control the ROIs on ZDT1 and two different reference points $(0.4, 0.8)$, $(0.8, 0.8)$ and $\epsilon=(0.2, 0.2)$ on ZDT2. After 100 generations, the results of the first interaction ($H=1$) on ZDT1 and ZDT2, are shown in the second row in Figs. 8 and 9 respectively. In Fig. 8, the ROIs are distributed in both ends; in Fig. 9, the ROIs are mixed together except the first plot obtained by MOEA/D-a.

After that, more specific preference information will be presented. On ZDT1, reference points like $(1.1, 0.1)$, $(0.1, 0.9)$ and $\epsilon=(0.1, 0.1)$ are set in the second interaction stage ($H=2$); on ZDT2, $\epsilon=(0.1, 0.1)$ is provided to divide the ROIs with the same reference points in the first stage. The third row in both figures shows the different obtained ROIs by MOEA/D-a, MOEA/D-b and MOEA/D-c in the second stage ($H=2$). It can be found that all of the obtained ROIs are narrowed and divided.

In order to get more accurate ROIs in the third interaction stage ($H=3$), on ZDT1, reference points $(0.6, 0.2)$, $(0.2, 0.6)$ with $\epsilon=(0.1, 0.1)$ are specified; on ZDT2, $\epsilon=(0.01, 0.01)$ is presented. The last row in Fig. 8 presents the final ROIs obtained by the three approaches in both figures, where more specific ROIs have been obtained by MOEA/D-a, MOEA/D-b and MOEA/D-c finally.

From the above experiments, we can prove the feasibility of this new approaches initially since they could find the ROIs according to the varying preference information of the DM. Besides, the results on 2-objective MOPs indicate that MOEA/D-a, MOEA/D-b and MOEA/D-c have the ability in solving 2-objective optimization problems well.

5.3. Results on 3-objective MOPs

In this section, 3-objective MOPs DTLZ1 and DTLZ2 [41] will be used to test the ability of the proposed procedures to solve 3-objective problems.

The 7-variable DTLZ1 is discussed here, and its PF is $\sum_{i=1}^m f_i = 0.5$, which is a geometric plane with 0.5 as the maximum value in each objective. DTLZ1 is defined as follows:

$$\text{Minimize} \begin{cases} f_1(X) = \frac{1}{2}x_1x_2\cdots x_{m-1}(1+g(\chi_m)), \\ f_2(X) = \frac{1}{2}x_1x_2\cdots (1-x_{m-1})(1+g(\chi_m)), \\ \dots \\ f_{m-1}(X) = \frac{1}{2}x_1(1-x_2)(1+g(\chi_m)), \\ f_m(X) = \frac{1}{2}(1-x_1)(1+g(\chi_m)) \end{cases} \quad (8)$$

where

$$X = (x_1, \dots, x_{m-1}, x_m, \dots, x_n),$$

$$\chi_m = (x_m, \dots, x_n), 0 \leq x_i \leq 1, i = \{1, \dots, n\}$$

$$g(\chi_m) = 100[|\chi_m| + \sum_{x_i \in \chi_m} (x_i - 0.5)^2 - \cos(20\pi(x_i - 0.5))].$$

Here, m is the number of objectives, and n is the number of variables. (m, n) is set to be $(3, 7)$ in the experiment.

The 12-variable DTLZ2 problem has a three-dimensional, non-convex, Pareto-optimal frontier, and its PF satisfies $\sum_{i=1}^m (f_i)^2 = 1$. It is illustrated as follows:

$$\text{Minimize} \begin{cases} f_1(X) = (1+g(\chi_m)) \cos(x_1\pi/2)\cdots \cos(x_{m-2}\pi/2)\cos(x_{m-1}\pi/2), \\ f_2(X) = (1+g(\chi_m)) \cos(x_1\pi/2)\cdots \cos(x_{m-2}\pi/2)\sin(x_{m-1}\pi/2), \\ f_3(X) = (1+g(\chi_m)) \cos(x_1\pi/2)\cdots \sin(x_{m-2}\pi/2), \\ \dots \\ f_m(X) = (1+g(\chi_m)) \sin(x_1\pi/2) \end{cases}$$

where

$$X = (x_1, \dots, x_{m-1}, x_m, \dots, x_n),$$

$$\chi_m = (x_m, \dots, x_n), 0 \leq x_i \leq 1, i = \{1, \dots, n\}$$

$$g(\chi_m) = \sum_{x_i \in \chi_m} (x_i - 0.5)^2.$$

Here, m is the number of objectives, and n is the number of variables. (m, n) is set to be $(3, 12)$ in that experiment.

5.3.1. Results on DTLZ1 and DTLZ2

Figs. 10 and 11 present the results obtained by three procedures on DTLZ1 and DTLZ2 in different stages.

At the preparation stage ($H=0$), as shown in the first row in Figs. 10 and 11, all of the obtained solutions spread over the entire Pareto front after the preparation with 200 generations, since there is no preference information to guide the searching process.

In the first interaction stage ($H=1$), DM specifies his/her preference information during the optimization process. On DTLZ1, the reference points $(0.05, 0.05, 0.5)$, $(0.5, 0.05, 0.05)$ and $(0.05, 0.5, 0.05)$, and the range of ROIs $\epsilon=(0.2, 0.2, 0.2)$ are given. On DTLZ2, the reference points $(0.2, 0.4, 0.6)$, $(0.4, 0.6, 0.2)$, $(0.6, 0.2, 0.4)$ and $\epsilon=(0.2, 0.2, 0.2)$ are specified to detect the desired regions. After 100 generations, the plots in the second row present the outcomes in response to the preference information. In Fig. 10, the obtained ROIs are close to the corners of the PF, which makes the DM learn more information about the range of the PF of the problem. In Fig. 11, it can be seen that the obtained ROIs are too large, because the range of ROIs are set as $\epsilon=(0.2, 0.2, 0.2)$.

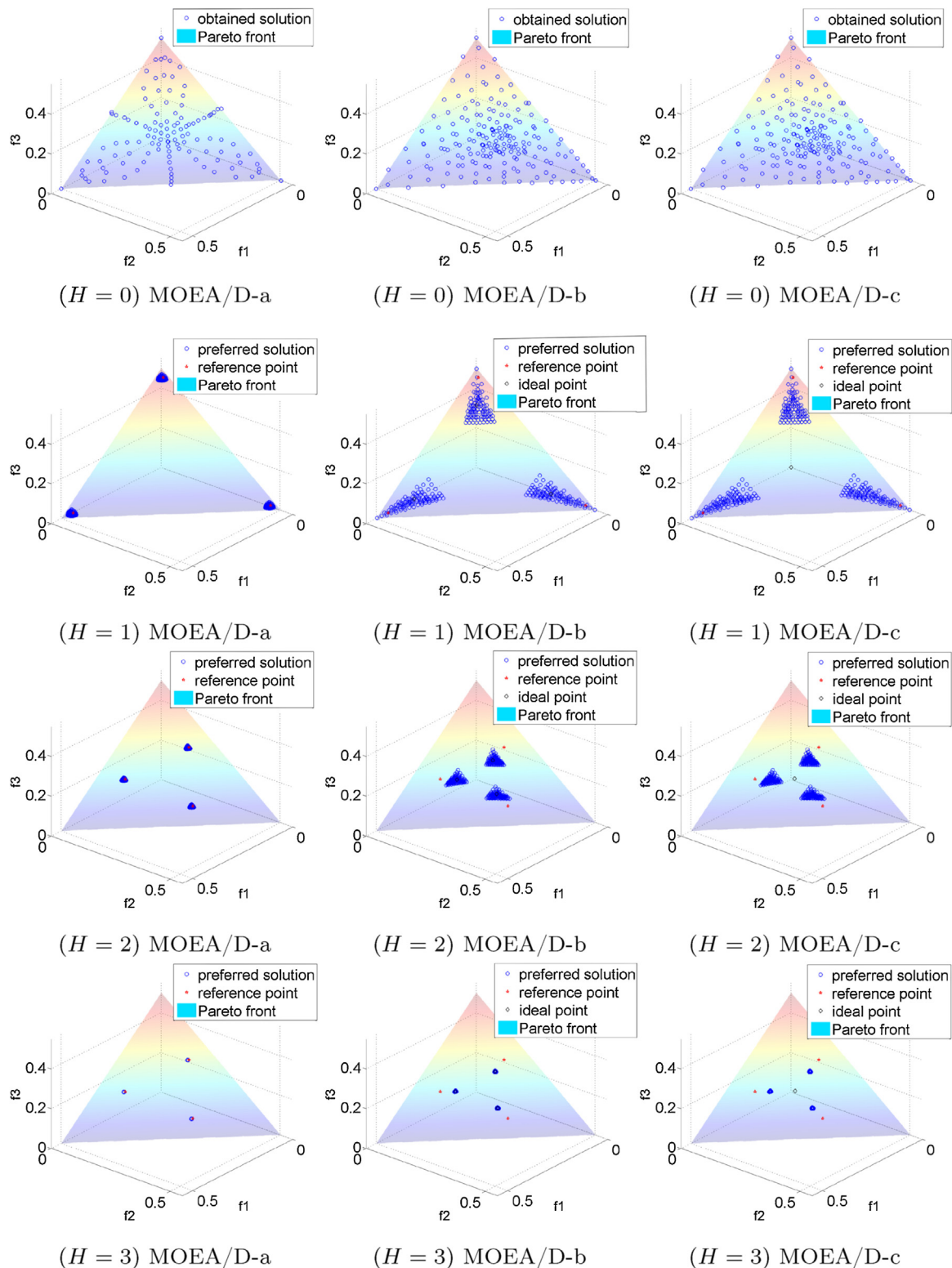
Thereby, the next interaction ($H=2$) is to modify the preference information slightly and guide the searching process to more specific ROIs. On DTLZ1, the reference points are specified like $(0.1, 0.2, 0.3)$, $(0.2, 0.3, 0.1)$, $(0.3, 0.1, 0.2)$ and $\epsilon=(0.1, 0.1, 0.1)$ are specified; on DTLZ2, the reference points are set to be $(0.1, 0.2, 1.1)$, $(0.8, 0.1, 0.2)$, $(0.2, 1.1, 0.1)$ and $\epsilon=(0.1, 0.1, 0.1)$. In Figs. 10 and 11, it could be found that the ROIs in 3rd row turn to be smaller and focused to the reference points.

In the last interaction ($H=3$), more specific preference information $\epsilon=(0.01, 0.01)$ is set on DTLZ1 and DTLZ2. From the 4th row in both figures, we could find that the ROIs close to the reference points have been obtained finally in according to the preference information.

Thus, after four stages interactive searching process, the proposed approaches are able to find the proper ROIs for the DM on dealing with 3-objective problems.

5.4. Results on many-objective MOPs

On dealing with many-objective problems, it is not only challenging to search the entire objective space but also potentially can waste lots of computing resources. Thus, the interactive approaches are always devoted to searching the ROIs or desired solutions for the DM, hence should be more effective and efficient. In this section, we will test the ability of the proposed approaches to deal with many-objective problems during the interactive process, and

**Fig. 10.** Results on DTLZ1 obtained MOEA/D-a, MOEA/D-b and MOEA/D-c in different stages.

the 10-objective and 15-objective DTLZ2 are selected to be the test instances.

5.4.1. On DTLZ2 with 10 objectives

In this section, the (m, n) of DTLZ2 is set as $(10, 19)$. Its Pareto-optimal solutions satisfy $\sum_{i=1}^m (f_i)^2 = 1$. The results

obtained by MOEA/D-a, MOEA/D-b and MOEA/D-c are shown in Fig. 12.

$$\begin{cases} A = (0.30, 0.30, 0.10, 0.30, 0.55, 0.35, 0.35, 0.35, 0.25, 0.45) \\ B = (0.60, 0.65, 0.60, 0.60, 0.80, 0.50, 0.50, 0.55, 0.55, 0.55) \end{cases} \quad (9)$$

In Fig. 12, each black solid line stands for an individual, and the reference points are marked with red dashed lines. The vertical

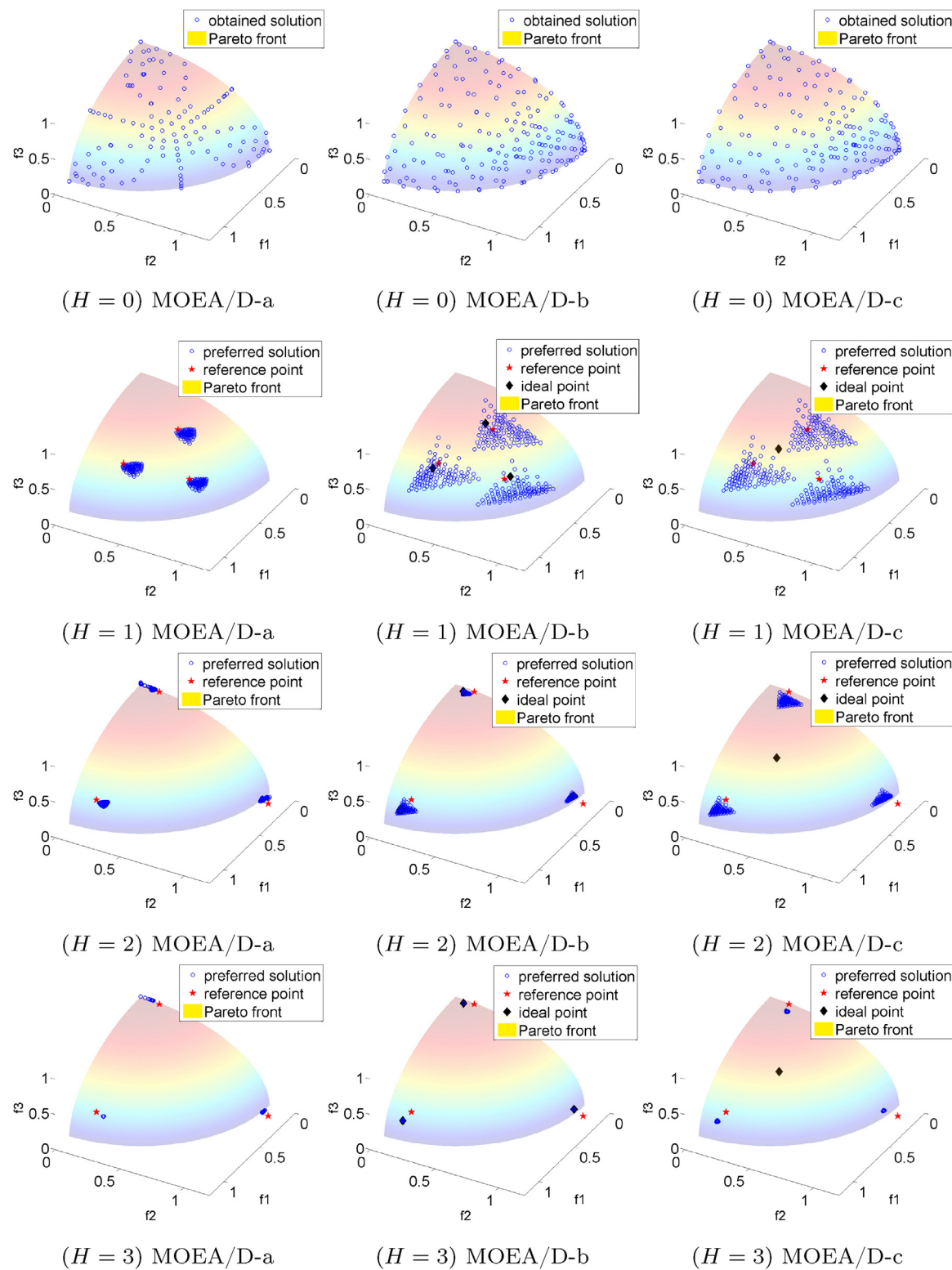
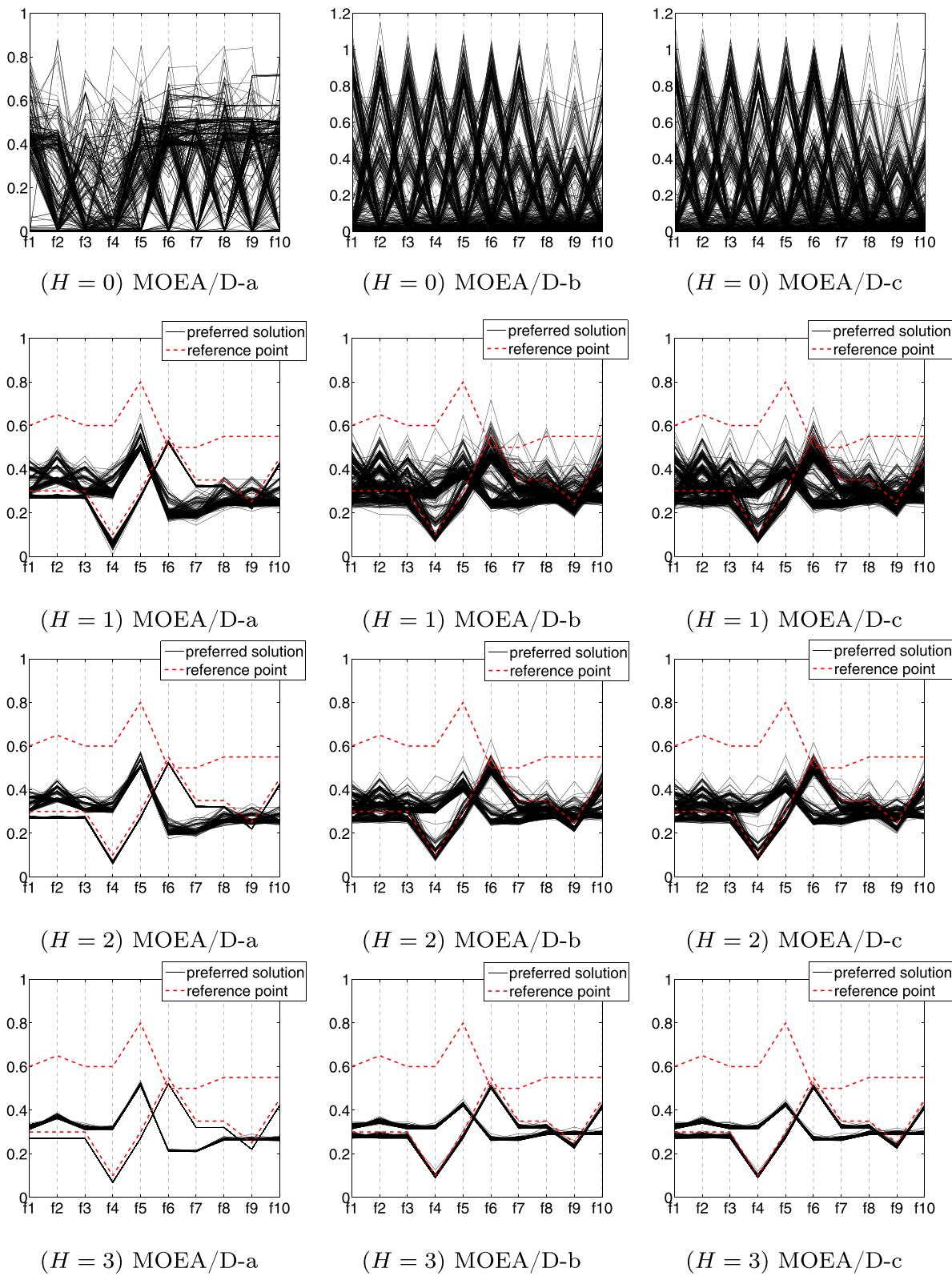


Fig. 11. Results on DTLZ2 obtained MOEA/D-a, MOEA/D-b and MOEA/D-c in different stages.

coordinate shows the solution's objective values. At the preparation stage with 200 generations, the first row in Fig. 12 shows that the individuals are difficult to converge without guidance of preference information. In the first interaction stage, the reference points are presented in Eq. (9), and every component in ϵ is set to be 0.1 to control the range of ROIs. Notably, $\sum_{i=1}^m (f_i(A))^2 = 1.178$ and $\sum_{i=1}^m (f_i(B))^2 = 3.55$, which means that both of the reference

points A and B are in the feasible objective space. A is very close to the PF but B is comparatively farther away from the PF because the Pareto-optimal solutions of DTLZ2 satisfy $\sum_{i=1}^m (f_i)^2 = 1$. The second row shows the results of the second stage with the first interaction. Only in the first plot, we can distinguish the ROIs belonging to which reference points. Thus, the second interaction will narrow the ROIs by setting each component of ϵ as

**Fig. 12.** Results on 10-objective DTLZ2 obtained MOEA/D-a, MOEA/D-b and MOEA/D-c in different stages.

0.05. The plots in the third row show that the boundaries of the ROIs turn to be clear after the interaction. In the last stage, more focused preference information will be provided, and the components in ϵ are set as 0.01. It is apparent from the last row in Fig. 12 that the boundaries of the ROIs are entirely clear. Besides, the $\sum_{i=1}^m (f_i)^2$ values of all solutions are among (1.000549,

4.39E-09),² (1.000012, 1.20E-12), and (1.000012, 1.18E-12) obtained by MOEA/D-a, MOEA/D-b and MOEA/D-c respectively,

² (average, variance): the first value is the average value of the $\sum_{i=1}^m (f_i)^2$; the second one is the corresponding variance value.

which demonstrates that all of the obtained solutions have converged into the PF and close to the reference points.

From the experiment above, the proposed approaches have been demonstrated to have the ability to deal with many-objective problem.

5.4.2. On DTLZ2 with 15 objectives

In this section, the (m, n) of DTLZ2 is set as $(15, 24)$. Also the PF satisfies $\sum_{i=1}^m (f_i)^2 = 1$. The results obtained by the proposed procedures are shown in Fig. 13.

$$\left\{ \begin{array}{l} A = (0.80, 0.80, 0.60, 0.90, 0.70, 0.70, 0.60, 0.90, 0.60, 0.70, 0.70, 0.60, 0.80, 0.80, 0.80) \\ B = (0.30, 0.30, 0.30, 0.10, 0.30, 0.30, 0.30, 0.50, 0.20, 0.30, 0.10, 0.45, 0.10, 0.20, 0.20) \end{array} \right. \quad (10)$$

In Fig. 13, solutions in the preparation stage do not converge into the PF. From the plots, some objective values of the solutions are bigger than 1.0. In the first interaction stage ($H=1$), two different reference points are given in Eq. (10), and the value of each component in ϵ is set to be 0.1 to control the ranges of ROIs. From second row, the obtained ROIs are completely mixed and hard to differentiate. So the task of the next interaction stage is to separate those ROIs, thereby the component of ϵ is set to be 0.05. Although more specific preference information is provided to guide the searching process, the results shown in third row in Fig. 13 are still intermixed and hard to separate them apart. The last interaction provides even smaller value (0.01) of the component of ϵ . It is obvious from the 4th row in Fig. 13 that two different ROIs are obtained. Notably, the $\sum_{i=1}^m (f_i)^2$ values of all solutions are among $(1.001479, 2.03E-06)$, $(1.000018, 4.90E-12)$ and $(1.000018, 2.71E-12)$ obtained by MOEA/D-a, MOEA/D-b and MOEA/D-c respectively, which means that the obtained solutions are very close to the PF. From the plots, it can be found that the obtained ROIs have similar shapes as the reference point, which means that the obtained ROIs are close to the reference points.

From the experimental results, we could see that MOEA/D-a, MOEA/D-b and MOEA/D-c all have the ability to deal with many-objective problems well during the multiple preference-based interactive process.

5.5. Comparative results between the proposed approaches and MOEA/D

$$\begin{aligned} \Re_1 &= \left(\begin{array}{cccccccccccc} 0.30 & 0.30 & 0.10 & 0.30 & 0.55 & 0.35 & 0.35 & 0.35 & 0.25 & 0.45 \\ 0.60 & 0.65 & 0.60 & 0.60 & 0.80 & 0.50 & 0.50 & 0.55 & 0.55 & 0.55 \\ 0.50 & 0.40 & 0.30 & 0.60 & 0.45 & 0.35 & 0.45 & 0.45 & 0.45 & 0.45 \\ 0.70 & 0.75 & 0.50 & 0.60 & 0.50 & 0.50 & 0.50 & 0.55 & 0.55 & 0.55 \\ 0.10 & 0.30 & 0.20 & 0.30 & 0.55 & 0.35 & 0.45 & 0.35 & 0.55 & 0.25 \\ 0.65 & 0.85 & 0.40 & 0.40 & 0.50 & 0.45 & 0.50 & 0.55 & 0.55 & 0.35 \\ 0.45 & 0.45 & 0.50 & 0.45 & 0.55 & 0.35 & 0.55 & 0.75 & 0.85 & 0.35 \\ 0.20 & 0.20 & 0.10 & 0.25 & 0.15 & 0.35 & 0.45 & 0.55 & 0.25 & 0.45 \\ 0.60 & 0.30 & 0.15 & 0.60 & 0.25 & 0.75 & 0.25 & 0.55 & 0.65 & 0.25 \\ 0.75 & 0.35 & 0.20 & 0.60 & 0.55 & 0.25 & 0.55 & 0.35 & 0.75 & 0.85 \end{array} \right) \\ \Re_2 &= \left(\begin{array}{cccccccccccc} 0.80 & 0.80 & 0.60 & 0.90 & 0.70 & 0.70 & 0.60 & 0.90 & 0.60 & 0.70 & 0.70 & 0.60 & 0.80 & 0.80 & 0.80 \\ 0.30 & 0.30 & 0.30 & 0.10 & 0.30 & 0.30 & 0.30 & 0.50 & 0.20 & 0.30 & 0.10 & 0.45 & 0.10 & 0.20 & 0.20 \\ 0.50 & 0.40 & 0.30 & 0.60 & 0.45 & 0.35 & 0.45 & 0.45 & 0.45 & 0.45 & 0.60 & 0.90 & 0.70 & 0.70 & 0.60 \\ 0.70 & 0.75 & 0.50 & 0.60 & 0.50 & 0.50 & 0.50 & 0.55 & 0.55 & 0.55 & 0.60 & 0.70 & 0.70 & 0.60 & 0.80 \\ 0.10 & 0.30 & 0.20 & 0.30 & 0.55 & 0.35 & 0.45 & 0.35 & 0.55 & 0.25 & 0.80 & 0.60 & 0.90 & 0.70 & 0.70 \\ 0.65 & 0.85 & 0.40 & 0.40 & 0.50 & 0.45 & 0.50 & 0.55 & 0.55 & 0.35 & 0.70 & 0.60 & 0.80 & 0.80 & 0.80 \\ 0.45 & 0.45 & 0.50 & 0.45 & 0.55 & 0.35 & 0.55 & 0.75 & 0.85 & 0.35 & 0.20 & 0.20 & 0.10 & 0.25 & 0.15 \\ 0.20 & 0.20 & 0.10 & 0.25 & 0.15 & 0.35 & 0.45 & 0.55 & 0.25 & 0.45 & 0.50 & 0.60 & 0.50 & 0.50 & 0.50 \\ 0.60 & 0.30 & 0.15 & 0.60 & 0.25 & 0.75 & 0.25 & 0.55 & 0.65 & 0.25 & 0.75 & 0.35 & 0.20 & 0.60 & 0.55 \\ 0.75 & 0.35 & 0.20 & 0.60 & 0.55 & 0.25 & 0.55 & 0.35 & 0.75 & 0.85 & 0.30 & 0.30 & 0.10 & 0.30 & 0.55 \end{array} \right) \end{aligned}$$

In this section, we compare the convergence ability of the proposed approaches and the Tchebycheff approach based MOEA/D on 10-objective and 15-objective DTLZ2 respectively. All of the experiments are conducted 30 runs independently to demonstrate the performance of the proposed approaches. We conduct the 10-objective experiments with 2, 5, 8 and 10 reference points, and the matrix of 10 reference points is shown in \Re_1 . In the matrix, each line represents one reference point. Each experiment takes the required number of reference points in the matrix from the top line to the

designated line. For example, for the experiment with 5 reference points, the first 5 lines in the \Re_1 are the chosen reference points. Similarly, we also conduct the 15-objective experiments with 2, 5, 8 and 10 reference points as shown in \Re_2 . The value of each component in ϵ is set to be 0.01 to control the ranges of ROIs in these two set of experiments. The termination conditions is 500 generations which equals 2.5×10^5 evaluations.

Fig. 14 presents the results obtained by MOEA/D-a, MOEA/D-b, MOEA/D-c and MOEA/D. The GD in the label of the vertical coordinates is the generation distance (GD) which is defined as $GD = \sum_{i=1}^m (f_i)^2$, since the Pareto-optimal set of DTLZ2 satisfies $\sum_{i=1}^m (f_i)^2 = 1$. In other words, the smaller the GD value is, the better convergence the algorithm obtains.

From Fig. 14, it is obvious that the GD values obtained by MOEA/D-a, MOEA/D-b, MOEA/D-c are smaller than that obtained by MOEA/D. The performances of MOEA/D-b and MOEA/D-c are similar and rank the first. With the guidance of preference information, at the beginning of process from 0 to 0.5×10^5 evaluations, the obtained solutions are swiftly approximating to the Pareto-optimal front. Then it keeps a descending tendency until the end of the optimization. MOEA/D-a ranks the second, and it has the same trend but changes less shapely.

For MOEA/D-b and MOEA/D-c, it can be seen from Fig. 14 that the Y-axis values of MOEA/D-b and MOEA/D-c almost reach to -5 on

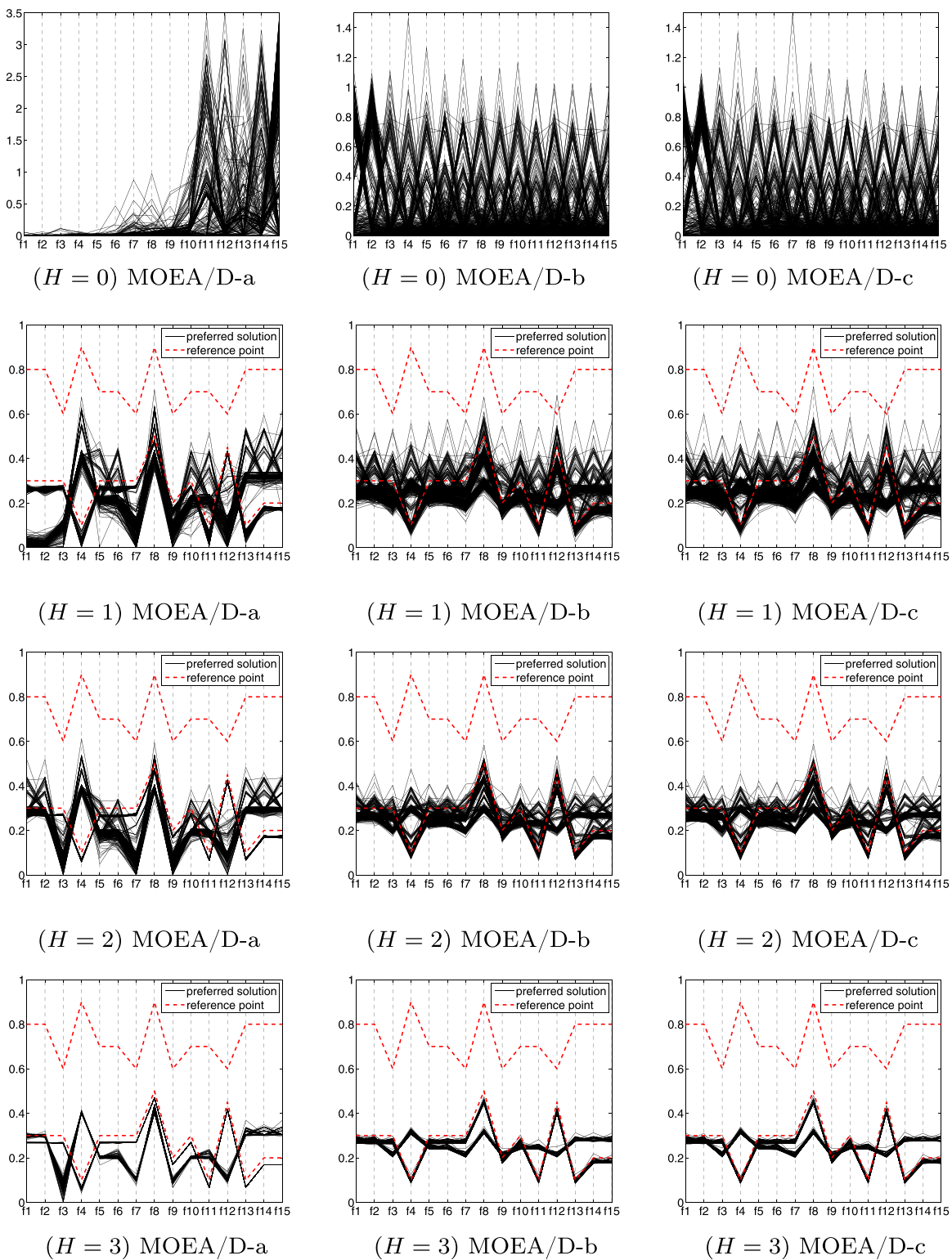


Fig. 13. Results on 15-objective DTLZ2 obtained MOEA/D-a, MOEA/D-b and MOEA/D-c in different stages.

the experiments with 2 and 5 reference points like Fig. 14(a), (e), (b) and (f). But the Y-axis values tend to be -4 on the experiments with 8 and 10 reference points like Fig. 14(c), (g), (d) and (h). It means that the performance of MOEA/D-b and MOEA/D-c will degenerate with the increase of the number of reference points. The reason is that more reference points will lead to smaller sub-population and less computational resources spent on one sub-population.

When dealing with the problems with 5 and 10 reference points, the performance of MOEA/D-a tends to be less effective than that of MOEA/D-b and MOEA/D-c. The reason is that the ideal point tends to be located in the infeasible region and contributes to a more focused searching to guide the solutions to the ideal point. Meanwhile, the obtained solutions will reach to the ROI consequently. For MOEA/D-a, the solutions will be guided to the reference points

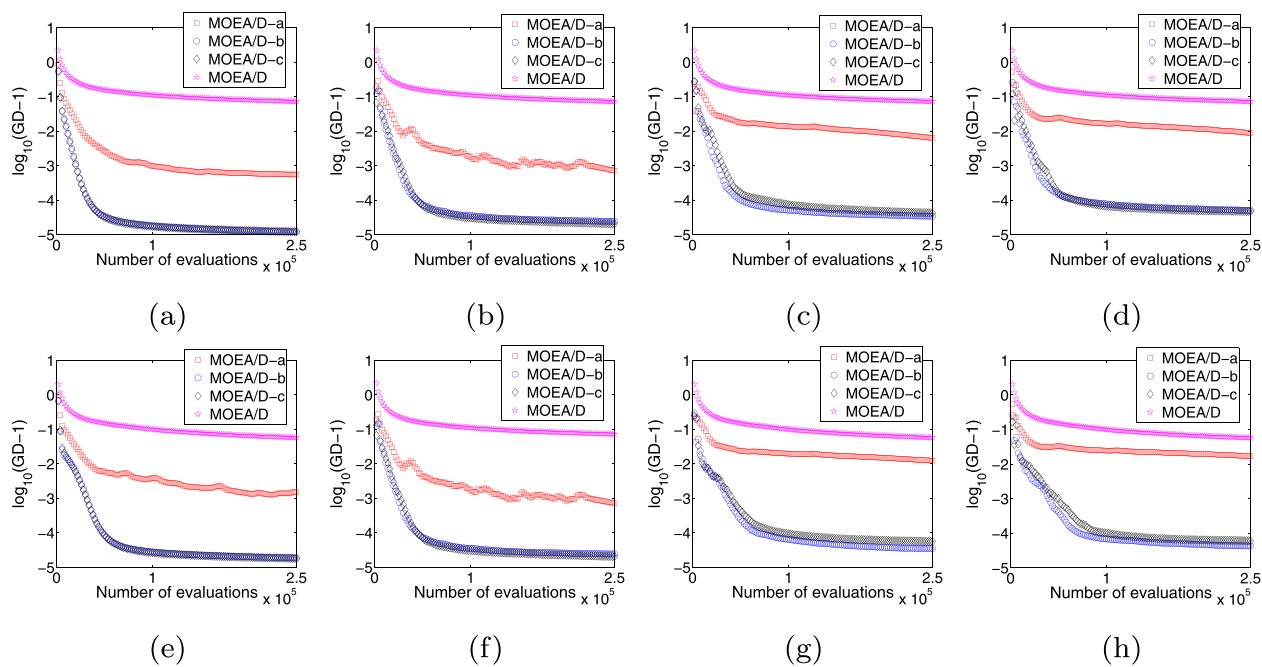


Fig. 14. The comparative results on 10- and 15-objective DTLZ2 between MOEA/D-a, MOEA/D-b, MOEA/D-c and MOEA/D. The first row and the second row are on 10- and 15-objective DTLZ2 with 2, 5, 8 and 10 reference points respectively.

as much as possible. Thus, when the reference point is located in the feasible region, the performance of MOEA/D-a will be less encouraging.

The Y-axis value of MOEA/D in the end reaches to -1 which means its GD values is around 1.1 , namely, some solutions still do not converge into the PF in the end. The reason is that MOEA/D has to search a set of Pareto-optimal solutions in such a high-dimensional objective space with limited computing resources. Additionally, the neighborhood mechanism loses the sharing of dominant gene. In other words, the subproblems cannot use the information of the elite solutions from the neighbor subproblems to prompt the optimization for themselves in a high-dimensional space. Thus, it cannot converge soon.

Thus, from the experiments with different amount of reference points, a conclusion can be made that with the guidance of preference information, MOEA/D-a, MOEA/D-b, MOEA/D-c could save much computational resources to find the well-converged ROIs for the DM rather than the whole PF. Also, the performance of the proposed algorithms will degenerate to some extent with the increase of the number of reference points. Thus, less number of reference points will be beneficial and more effective during the optimization.

5.6. Comparative experiments

In this section, we conduct a set of experiments to demonstrate the ability of the proposed approaches to deal with multi- and many-objectively problems in comparison with other three reference point based EMO algorithms: g-NSGA-II [31], r-NSGA-II [32], and IMOEA/D-PRE [36]. The sets of ZDT [40] and DTLZ [41] are considered as the test problems. The 5-objective, 8-objective, 10-objective DTLZ2 and DTLZ4 are chosen to be the many-objective test problems.

In all simulations, the distribution index of simulated binary crossover operator and polynomial mutation is 10 and 20 respectively. The crossover probability and mutation probability are $P_c = 0.99$ and $P_m = 0.1$ respectively. About IMOEA/D-PRE and the three proposed approaches in the paper, T is 10, and the preset penalty parameter θ in PBI approach is set to be 5. Considering the r -dominance relation, δ is set to be 0.2. The range of the ROI is set to be 0.1 on 2-objective and 3-objective problems, and 0.05 for 5-, 8-, and 10-objective DTLZ2 and DTLZ4. On multi-objective problems, the setting of the reference points and relevant settings are shown in Table 1. On many-objective problems, the population size is 200, and the maximum generation is 500. The reference point is

Table 1

Parameter setting on ZDT and DTLZ problems. The reference points are set in the infeasible region and feasible region. The termination condition is the maximum generations. The population size is 100 and 200 for ZDT and DTLZ problems respectively. More generations are given on ZDT4 and ZDT6 because they are designed hard to approximate to the PF.

Instances	In infeasible region	In feasible region	Generations	Population
ZDT1	(0.10,0.20)	(0.40,0.55)	500	100
ZDT2	(0.10,0.20)	(0.70,0.80)	500	100
ZDT3	(0.10,0.20)	(0.40,0.40)	500	100
ZDT4	(0.10,0.20)	(0.50,0.50)	1500	100
ZDT6	(0.10,0.20)	(0.70,0.80)	1200	100
DTLZ1	(0.10,0.20,0.10)	(0.25,0.25,0.25)	500	200
DTLZ2	(0.10,0.20,0.10)	(0.80,0.80,0.80)	500	200
DTLZ3	(0.10,0.20,0.10)	(0.80,0.80,0.80)	500	200
DTLZ4	(0.10,0.20,0.10)	(0.60,0.60,0.80)	500	200
DTLZ5	(0.10,0.20,0.10)	(0.70,0.70,0.90)	500	200
DTLZ6	(0.10,0.20,0.10)	(0.70,0.60,0.60)	500	200

Table 2

The GD values of the solutions obtained by MOEA/D-a, MOEA/D-b, MOEA/D-c, g-NSGA-II, r-NSGA-II, and IMOEA/D-PRE on the set of ZDT and DTLZ problems. The best and second best values are highlighted with deep gray background and gray background respectively.

Instances	g-NSGA-II	r-NSGA-II	IMOEA/D-PRE	MOEA/D-a	MOEA/D-b	MOEA/D-c
The reference point in the infeasible region						
ZDT1	2.23E-04† 5.54E-09†	5.70E-05 4.47E-09	5.75E-05 3.38E-11	4.40E-05 3.02E-11	8.23E-05 3.02E-08	1.62E-04† 9.57E-13†
ZDT2	3.85E-04† 3.31E-08†	1.37E-04† 1.04E-08†	9.79E-05 4.52E-11	6.96E-05 3.49E-10	2.95E-05 4.72E-12	2.87E-05 2.22E-12
ZDT3	7.81E-04 2.65E-07	1.88E-04 9.86E-08	2.17E-02† 2.28E-13†	1.96E-04 3.22E-09	1.67E-04 5.23E-11	1.69E-04 8.15E-11
ZDT4	2.85E-01† 1.14E-01†	2.37E-01† 1.54E-02†	5.72E-05 2.25E-11	1.29E-03† 3.14E-07†	4.75E-04 3.99E-08	3.81E-04 2.98E-08
ZDT6	8.06E-03† 1.41E-04†	9.46E-04 7.51E-06	1.02E-04 3.02E-11	2.64E-03† 9.76E-06†	1.89E-04 3.46E-11	1.90E-04 4.98E-11
The reference point in the feasible region						
ZDT1	6.04E-05 2.41E-10	3.90E-05 1.46E-09	5.75E-05 2.81E-11	4.72E-05 1.84E-10	3.94E-05 1.83E-11	4.08E-05 1.76E-11
ZDT2	7.72E-05 5.73E-10	3.45E-05 2.11E-09	9.99E-05 7.61E-11	5.58E-05 1.14E-10	4.13E-05 1.29E-11	4.17E-05 7.74E-12
ZDT3	2.30E-05 1.12E-11	2.37E-05 1.60E-10	2.22E-02† 2.51E-13†	1.57E-02† 2.38E-05†	4.95E-05 9.91E-10	3.88E-05 2.92E-10
ZDT4	5.15E-01† 1.00E-01†	2.05E-01† 2.50E-02†	6.21E-05 1.25E-11	1.72E-03† 8.34E-07†	6.08E-04 1.14E-07	1.32E-03† 6.08E-06†
ZDT6	8.34E-03† 1.71E-04†	8.18E-05 7.51E-11	8.84E-05 1.98E-11	6.55E-03† 2.79E-05†	4.15E-04 1.47E-08	4.28E-04 1.13E-08
The reference point in the infeasible region						
DTLZ1	6.67E-00† 2.70E-00†	9.51E-03† 3.69E-04†	1.72E-04 3.25E-11	1.65E-04 2.17E-13	1.62E-04 6.72E-13	1.63E-04 9.57E-13
DTLZ2	3.85E-04 1.06E-03	1.37E-04 5.52E-04	9.79E-05 6.63E-04	4.40E-04 8.74E-12	4.51E-04 1.74E-11	4.51E-04 1.94E-11
DTLZ3	1.51E+01† 2.69E+01†	1.74E-02† 1.98E-03†	4.30E-03 2.00E-04	8.86E-04 8.15E-09	9.51E-04 1.39E-07	8.31E-04 2.83E-10
DTLZ4	8.82E-04 7.51E-08	5.51E-04 6.86E-09	6.62E-04 1.92E-10	2.33E-03 1.11E-08	2.41E-03 1.44E-09	2.40E-03 2.66E-09
DTLZ5	3.61E-04 5.05E-10	3.62E-04 2.44E-10	1.49E-04 2.83E-11	1.17E-04 4.99E-14	1.48E-04 1.03E-13	1.49E-04 1.06E-13
DTLZ6	6.04E-02† 7.52E-04†	4.93E-02† 5.30E-04†	4.26E-04 4.97E-11	3.77E-04 6.54E-15	4.27E-04 9.84E-16	4.26E-04 1.58E-15
The reference point in the feasible region						
DTLZ1	4.93E-00† 1.71E-04†	1.73E-03† 2.75E-05†	1.77E-04 4.93E-11	1.62E-04 4.75E-13	1.58E-04 5.94E-13	1.60E-04 1.19E-12
DTLZ2	7.81E-04 2.52E-09	7.57E-05 2.51E-10	6.69E-04 2.14E-10	4.26E-04 1.28E-12	4.18E-04 1.44E-11	4.19E-04 1.39E-11
DTLZ3	1.82E+01† 1.65E+01†	1.28E-02† 3.97E-03†	8.76E-04 1.29E-06	7.61E-04 1.06E-09	8.05E-04 9.64E-10	8.02E-04 3.26E-10
DTLZ4	3.12E-04 7.70E-09	2.53E-04 2.99E-09	6.16E-04 2.83E-10	9.91E-04 4.10E-11	2.68E-03 4.69E-08	2.56E-03 1.36E-07
DTLZ5	1.12E-04 2.71E-10	6.20E-06 4.16E-11	1.31E-04 3.35E-11	1.54E-04 4.90E-15	1.34E-04 2.97E-13	1.34E-04 2.31E-13
DTLZ6	5.72E-03† 1.27E-06†	3.98E-03† 3.28E-06†	4.57E-04 5.39E-11	1.69E-04 1.27E-18	4.45E-04 2.52E-16	4.46E-04 3.71E-16

(0.1, 0.3, 0.2, 0.4, 0.2) on 5-objective problems, (0.3, 0.3, 0.3, 0.1, 0.3, 0.55, 0.35, 0.35) on 8-objective problems, and (0.3, 0.3, 0.3, 0.1, 0.3, 0.55, 0.35, 0.35, 0.25, 0.45) on 10-objective problems.

The indicators adopted in this section are the GD [42], and HV-UM [43] to evaluate the convergence and comprehensive performance of the solutions obtained by the algorithms. The smaller the GD value, the better convergence the algorithm obtains. The bigger HV-UM values means better comprehensive performance obtained by the algorithm. Besides, $\sum_{i=1}^m f_i^2$ is used to evaluate the convergence of the obtained solutions on many-objective problems, because the Pareto optimal solutions of DTLZ2 and DTLZ4 satisfy $\sum_{i=1}^m f_i^2 = 1$. Thus, the $\sum_{i=1}^m f_i^2$ value of the solutions obtained by an algorithm is closer to 1.0, and the convergence of the algorithm will be better. In Tables 2–7, the mean and standard deviation of the metric values are presented in the boxes, and the best and second best values are highlighted with deep gray background and gray background respectively. The symbol † on the top right

corner of the value indicates the remarkable p value (in Tamhane's T2 test [44]), and the significant level is 0.05.

5.6.1. On multi-objective problems

The experiments are conducted over 30 runs on two scenarios with the reference point in the infeasible region and in the feasible region, and the relevant settings are presented in Table 1.

The experimental results on multi-objective problems are shown in Tables 2 and 3. From Table 2, on ZDT problems, it can be seen that the number of the best GD values obtained by r-NSGA-II and IMOEA/D-PRE is most with 3 out of 10. MOEA/D-b obtains the most second best GD values with 5 records. Thus, from the GD values on ZDT problems, the convergence of the r-NSGA-II, MOEA/D-b, and IMOEA/D-PRE is better than that of others.

Interestingly, on ZDT4 and ZDT6 problems which are designed to be hard to search their true PFs, g-NSGA-II and r-NSGA-II are hard to converge into the true PFs under these two scenarios, because their

Table 3

The HV-UM values of the solutions obtained by MOEA/D-a, MOEA/D-b, MOEA/D-c, g-NSGA-II, r-NSGA-II, and IMOEA/D-PRE on the set of ZDT and DTLZ problems. δ in HV-UM is set to be 0.1. The best and second best values are highlighted with deep gray background and gray background respectively.

Instances	g-NSGA-II	r-NSGA-II	IMOEA/D-PRE	MOEA/D-a	MOEA/D-b	MOEA/D-c
The reference point in the infeasible region						
ZDT1	2.08E-01 2.61E-03	6.84E-01 3.14E-02	8.27E-01 7.13E-03	7.73E-01 1.28E-02	8.32E-01 2.03E-02	8.20E-01 1.40E-02
ZDT2	4.05E-01 1.65E-02	8.94E-01 3.36E-01	4.91E-01 4.62E-03	5.29E-01 1.89E-03	8.93E-03 [†] 4.68E-05 [†]	7.79E-03 [†] 2.48E-05 [†]
ZDT3	4.43E-02 5.65E-04	6.14E-02 4.25E-03	1.07E-01 2.39E-04	8.37E-02 1.04E-04	9.43E-02 2.55E-04	9.11E-02 1.95E-04
ZDT4	3.95E-01 [†] 1.74E-01 [†]	2.30E+00 2.64E+01	2.70E+00 3.36E+00	6.80E+00 1.02E+02	7.58E+00 1.93E+02	7.13E+00 1.86E+02
ZDT6	5.83E-01 2.71E-02	7.91E-01 3.73E-02	5.17E-01 2.23E-03	4.23E-01 2.23E-02	4.77E-01 2.26E-03	4.75E-01 2.46E-03
The reference point in the feasible region						
ZDT1	2.88E-01 1.41E-03	5.01E-01 2.21E-03	4.81E-01 2.36E-03	4.79E-01 2.39E-03	3.47E-01 7.12E-04	3.53E-01 1.04E-03
ZDT2	1.49E-01 1.44E-03	4.18E-01 1.66E-02	1.16E-01 3.91E-04	2.36E-01 6.66E-05	6.36E-01 1.51E-02	5.97E-01 1.86E-02
ZDT3	5.40E-01 2.89E-01	2.15E-02 5.47E-04	4.39E-02 3.43E-05	3.98E-03 [†] 2.02E-04 [†]	1.80E-02 3.99E-05	2.01E-02 3.18E-05
ZDT4	4.32E-03 [†] 1.68E-04 [†]	3.17E+01 5.38E+02	8.35E+01 1.38E+03	7.78E+01 1.41E+03	9.67E+01 1.49E+03	9.44E+01 1.54E+03
ZDT6	6.97E-01 4.66E-02	1.20E+00 2.67E-01	6.62E-01 5.25E-01	5.69E-01 1.06E+00	8.96E-01 9.12E-01	8.84E-01 9.64E-01
The reference point in the infeasible region						
DTLZ1	0.00E+00 [†] 0.00E+00 [†]	7.77E+01 [†] 9.43E+03 [†]	6.07E+02 5.93E+05	6.06E+02 5.97E+05	6.09E+02 5.94E+05	6.08E+02 5.94E+05
DTLZ2	3.32E-02 [†] 7.49E-04 [†]	2.04E-01 1.68E-02	4.59E-01 9.39E-02	1.86E-01 6.07E-03	5.43E-01 1.20E-01	5.23E-01 1.35E-01
DTLZ3	0.00E+00 [†] 0.00E+00 [†]	5.57E+01 [†] 2.88E+04 [†]	6.74E+02 2.92E+06	7.99E+02 5.89E+06	8.72E+02 5.64E+06	8.46E+02 5.14E+06
DTLZ4	5.48E-02 [†] 7.78E-03 [†]	7.53E-02 [†] 2.75E-03 [†]	3.64E-01 8.71E-02	2.03E-01 1.36E-02	4.81E-01 1.38E-01	5.09E-01 2.16E-01
DTLZ5	1.93E-02 1.91E-04	7.48E-02 3.27E-03	4.28E-02 2.37E-04	1.06E-01 3.82E-03	3.67E-02 2.84E-04	3.69E-02 2.85E-04
DTLZ6	7.61E-02 6.43E-03	8.19E-02 1.93E-02	7.82E-02 3.79E-03	1.74E-01 1.91E-02	8.56E-02 6.41E-03	8.80E-02 7.33E-03
The reference point in the feasible region						
DTLZ1	0.00E+00 [†] 0.00E+00 [†]	5.54E+02 [†] 3.90E+05 [†]	3.53E+03 1.47E+07	3.53E+03 1.47E+07	3.56E+03 1.47E+07	3.55E+03 1.47E+07
DTLZ2	3.90E-02 [†] 5.04E-04 [†]	6.45E-02 [†] 1.72E-03 [†]	2.82E-01 2.30E-02	1.94E-01 6.58E-03	3.14E-01 1.90E-02	3.30E-01 2.77E-02
DTLZ3	0.00E+00 [†] 0.00E+00 [†]	1.15E+03 [†] 2.11E+06 [†]	1.63E+04 4.11E+08	2.68E+04 1.11E+09	1.95E+04 6.38E+08	1.82E+04 5.04E+08
DTLZ4	6.51E-02 [†] 3.35E-03 [†]	7.88E-02 [†] 3.97E-03 [†]	2.51E-01 6.69E-02	5.39E-02 [†] 3.16E-03 [†]	2.90E-01 6.80E-02	2.87E-01 4.82E-02
DTLZ5	9.69E-02 [†] 5.03E-03 [†]	1.04E-01 2.36E-03	1.64E-01 2.69E-02	9.34E-02 [†] 5.94E-03 [†]	1.51E-01 2.47E-02	1.50E-01 2.61E-02
DTLZ6	1.99E-02 [†] 5.98E-04 [†]	1.16E-01 1.96E-02	3.46E-01 1.81E-01	3.28E-01 2.20E-01	3.60E-01 1.99E-01	3.70E-01 2.20E-01

GD values are bigger than 1.0E-02. However, the other approaches are able to converge to the PF of these two problems.

On DTLZ problems, MOEA/D-a, MOEA/D-b and r-NAGA-II have good performance. MOEA/D-a ranks the first with 4 best records.

The second is r-NSGA-II. But MOEA/D-b has the most highlighted values with 6 records. On dealing with 3-objective problems, g-NSGA-II and IMOEA/D-PRE are less effective than the others. Especially on DTLZ1 and DTLZ3 problems, the GD values obtained

Table 4

The $\sum_{i=1}^m f_i^2$ values of the solutions obtained by the MOEA/D-a, MOEA/D-b, MOEA/D-c, g-NSGA-II, r-NSGA-II, and IMOEA/D-PRE on and 5-, 8-, 10-, and 15-objective DTLZ problems. The best and second best values are highlighted with deep gray background and gray background respectively.

DTLZ2	5-objectives		8-objectives		10-objectives	
	Mean	Variance	Mean	Variance	Mean	Variance
g-NSGA-II	1.07986 [†]	1.07E-04 [†]	8.45629 [†]	1.95E-01 [†]	10.2882 [†]	8.68E-02 [†]
r-NSGA-II	1.00751 [†]	2.27E-06 [†]	1.01216 [†]	4.16E-06 [†]	1.12893 [†]	3.62E-05 [†]
IMOEA/D-PRE	1.00023 [†]	1.49E-09 [†]	1.00065 [†]	8.50E-09 [†]	1.00077 [†]	2.42E-08 [†]
MOEA/D-a	1.00261 [†]	2.92E-08 [†]	1.00048	1.98E-09	1.00047	6.41E-09
MOEA/D-b	1.000065	1.97E-11	1.000164	2.63E-10	1.00020	3.57E-10
MOEA/D-c	1.00005	2.38E-11	1.000161	2.83E-10	1.00019	3.36E-10

Table 5

The HV-UM values of the solutions obtained by the MOEA/D-a, MOEA/D-b, MOEA/D-c, g-NSGA-II, r-NSGA-II, and IMOEA/D-PRE on and 5-, 8-, 10-, and 15-objective DTLZ2 problems. δ in HV-UM is set to be 0.1. The best and second best values are highlighted with deep gray background and gray background respectively.

DTLZ2	5-objectives		8-objectives		10-objectives	
	Mean	Variance	Mean	Variance	Mean	Variance
g-NSGA-II	4.38E-05 [†]	3.25E-09 [†]	0.00E+00 [†]	0.00E+00 [†]	0.00E+00 [†]	0.00E+00 [†]
r-NSGA-II	2.93E-03 [†]	1.27E-05 [†]	1.73E-01	5.04E-02	1.82E-02	1.00E-03
IMOEA/D-PRE	4.11E-03	7.02E-06	1.21E-01	1.11E-02	1.51E-02	1.36E-02
MOEA/D-a	6.16E-05 [†]	7.90E-09 [†]	1.73E-01	5.58E-02	2.30E-02	1.24E-03
MOEA/D-b	3.69E-03	4.08E-06	1.74E-01	4.30E-02	2.32E-02	9.53E-04
MOEA/D-c	4.25E-03	6.44E-06	1.78E-01	4.57E-02	2.63E-02	9.34E-04

Table 6

The $\sum_{i=1}^m f_i^2$ values of the solutions obtained by the MOEA/D-a, MOEA/D-b, MOEA/D-c, g-NSGA-II, r-NSGA-II, and IMOEA/D-PRE on and 5-, 8-, 10-, and 15-objective DTLZ4 problems. The best and second best values are highlighted with deep gray background and gray background respectively.

DTLZ4	5-objectives		8-objectives		10-objectives	
	Mean	Variance	Mean	Variance	Mean	Variance
g-NSGA-II	1.09343 [†]	1.44E-04 [†]	7.71585 [†]	1.40E+00 [†]	9.30525 [†]	3.75E-01 [†]
r-NSGA-II	1.03744 [†]	2.37E-05 [†]	1.06433 [†]	5.82E-05 [†]	1.19756 [†]	3.97E-04 [†]
IMOEA/D-PRE	1.00082 [†]	1.15E-05 [†]	1.00132 [†]	5.07E-06 [†]	1.00139 [†]	4.00E-06 [†]
MOEA/D-a	1.00158 [†]	8.38E-07 [†]	1.00173 [†]	1.94E-06 [†]	1.00128 [†]	1.55E-06 [†]
MOEA/D-b	1.00006	9.42E-10	1.00041	2.40E-06	1.00048	7.67E-07
MOEA/D-c	1.00005	2.92E-09	1.00023	8.45E-08	1.00033	2.93E-07

by g-NSGA-II are more than 1.0, which indicates that the obtained solutions did not converge into the PF. Thus, on coping with 3-objective problems, MOEA/D-a, MOEA/D-b and r-NAGA-II have the better convergence than others.

Table 3 presents the HV-UM values of the solutions obtained by the algorithms. HV-UM metric is based on hypervolume (HV) to evaluate the comprehensive performance of the obtained solution from the convergence and the diversity. On multi-objective ZDT problems, both MOEA/D-b and r-NSGA-II got 4 best HV values, and they got twice and once second best records respectively, which denotes that these two algorithms outperform others on most of the two-objective ZDT problems on two scenarios. However, on three-objective DTLZ problems, it is obvious from the table that MOEA/D-b and MOEA/D-c have better performance than others because they got most best and second best values. MOEA/D-a also got 3 best values especially on DTLZ5 and DTLZ6 when the reference point is in the infeasible region.

In conclusion, in terms of **Tables 2 and 3**, r-NSGA-II and MOEA/D-b have better comprehensive performance on dealing with 2-objective problems, but MOEA/D-b and MOEA/D-c have better performance on 3-objective DTLZ problems.

5.6.2. On many-objective problems

In order to investigate the ability to deal with many-objective optimization problems, the typical continuous instance DTLZ2

and DTLZ4 with 5, 8, 10 objectives are adopted. We also evaluate the convergence performance of the algorithms in terms of $\sum_{i=1}^m f_i^2$ values and comprehensive performance according to HV-UM values, and all experiments are conducted over 30 independent runs.

Tables 4 and 6 present the $\sum_{i=1}^m f_i^2$ values of the solutions obtained by the six algorithms on DTLZ2 and DTLZ4 problems with 5, 8, 10 objectives. The best and second best values are highlighted. The $\sum_{i=1}^m f_i^2$ value closer to 1.0 is the better since the Pareto-optimal solutions of DTLZ2 and DTLZ4 satisfy $\sum_{i=1}^m f_i^2 = 1$. From these two tables, MOEA/D-b and MOEA/D-c outperform other four algorithms. In comparison with other algorithms, the convergence of the g-NSGA-II and r-NSGA-II degenerate much faster with the increase of the number of the objectives. The reason is that the enhanced Pareto-dominance in these two approaches hard distinguish the mutual relationship between the solutions in a high-dimensional space with the increase of the number of the objectives. The reason for MOEA/D-c better than MOEA/D-b in dealing with many-objective problems is that the ideal point of the entire population may give more convergence pressure to the solutions approximating to the ROIs.

Tables 5 and 7 present the HV-UM values of the solutions obtained by the six algorithms on DTLZ2 and DTLZ4 problems respectively. On DTLZ2 problems in **Table 5**, MOEA/D-b and MOEA/D-c have better performance on most of the problems. From

Table 7

The HV-UM values of the solutions obtained by the MOEA/D-a, MOEA/D-b, MOEA/D-c, g-NSGA-II, r-NSGA-II, and IMOEA/D-PRE on and 5-, 8-, 10-, and 15-objective DTLZ4 problems. δ in HV-UM is set to be 0.1. The best and second best values are highlighted with deep gray background and gray background respectively.

DTLZ4	5-objectives		8-objectives		10-objectives	
	Mean	Variance	Mean	Variance	Mean	Variance
g-NSGA-II	0.00E+00 [†]	0.00E+00 [†]	0.00E+00 [†]	0.00E+00 [†]	1.42E-04 [†]	3.48E-07
r-NSGA-II	4.69E-04 [†]	7.82E-07 [†]	3.57E-03 [†]	3.50E-05 [†]	6.62E-04 [†]	6.94E-07
IMOEA/D-PRE	1.17E-02	1.42E-04	5.87E-02	1.71E-02	2.39E-02	1.04E-03
MOEA/D-a	8.40E-04 [†]	2.69E-06 [†]	4.03E-02	5.76E-03	2.20E-02	1.77E-03
MOEA/D-b	9.64E-03	9.31E-05	7.69E-02	3.02E-02	1.27E-02	2.88E-04
MOEA/D-c	7.38E-03	2.54E-05	7.63E-02	2.79E-02	4.28E-02	9.29E-03

the table, g-NSGA-II is less effective to deal with many-objective problems with the increase of the number of objectives. 0.00E+00 denotes that there is no solution in the region of interest. Thus, the convergence pressure of g-NSGA-II is not enough than that of others. On DTLZ4 problems, IMOEA/D-PRE outperforms others on 5-objective DTLZ4. With the increase of the number of objectives,

the performance of MOEA/D-b and MOEA/D-c is better than that of others especially g-NSGA-II and r-NSGA-II. Thus, the ideal point in the aggregation based MOEA/D-b and MOEA/D-c could enhance the selection pressure, and the approach to generate weight vectors could promote the diversity of the solutions in the region of interest.

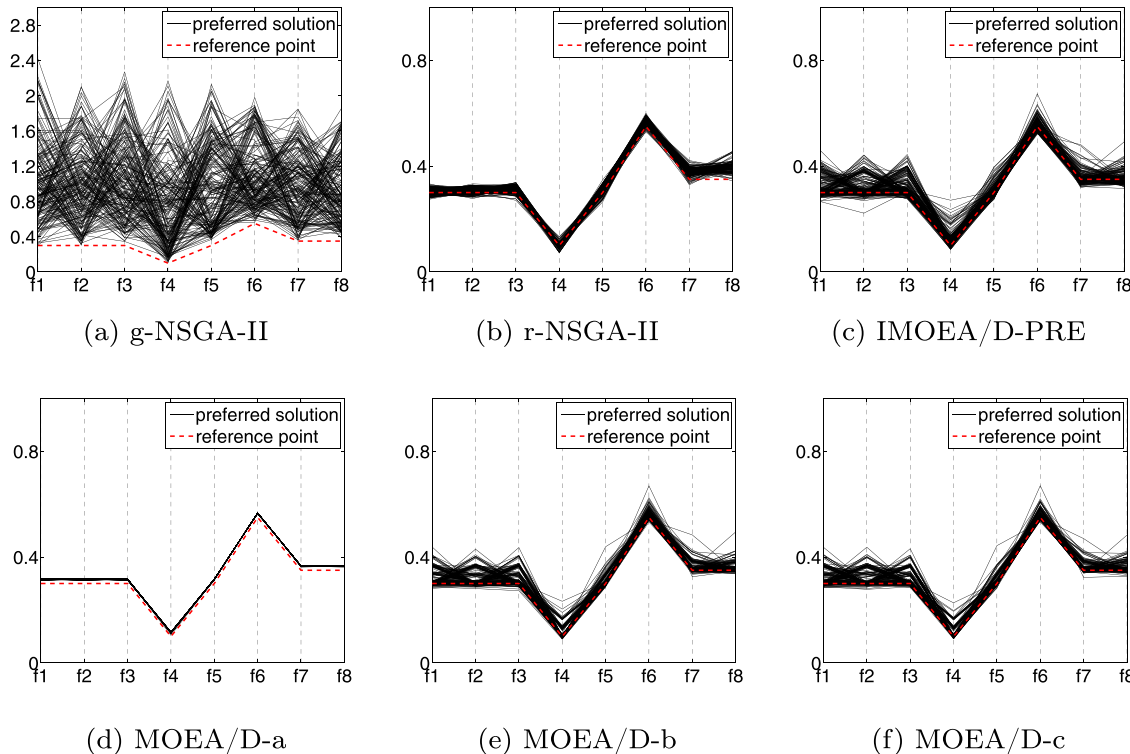


Fig. 15. Results on 8-objective DTLZ2 obtained g-NSGA-II, r-NSGA-II, IMOEA/D-PRE, MOEA/D-a, MOEA/D-b and MOEA/D-c.

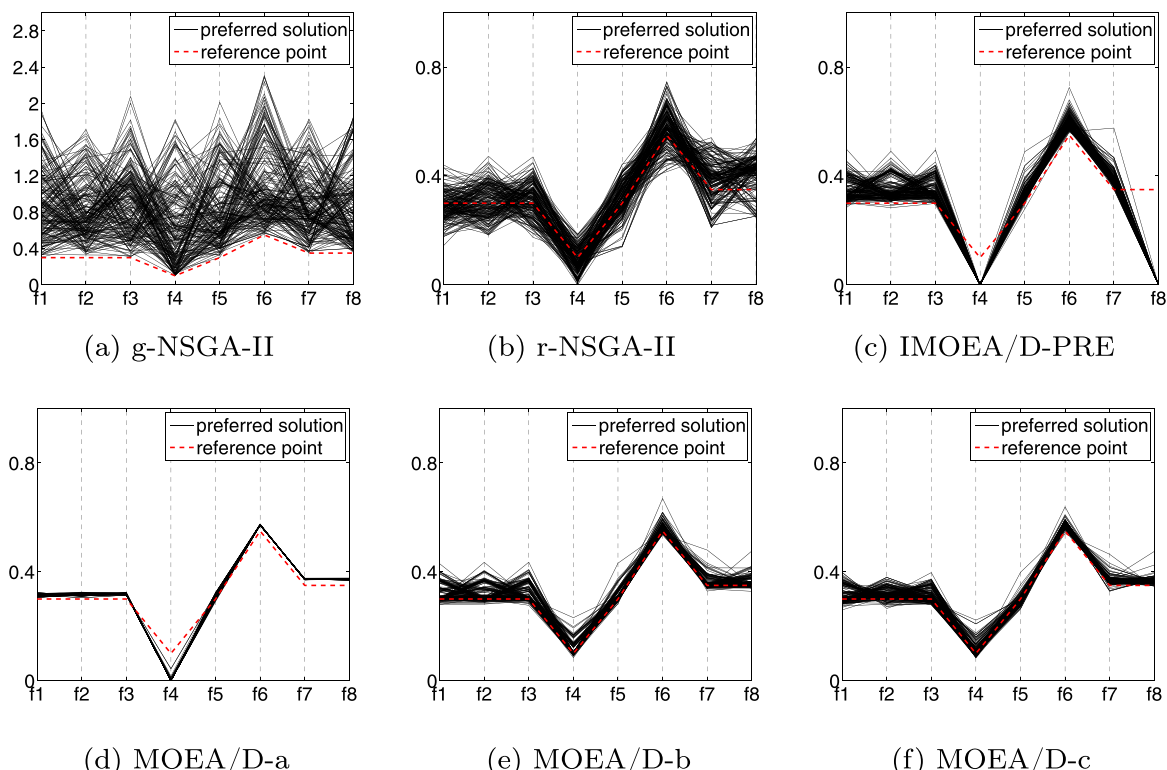


Fig. 16. Results on 8-objective DTLZ4 obtained g-NSGA-II, r-NSGA-II, IMOEA/D-PRE, MOEA/D-a, MOEA/D-b and MOEA/D-c.

Figs. 15 and 16 present the obtained solutions of the six algorithms on 8-objective DTLZ2 and DTLZ4 respectively. In Fig. 15(a), it can be seen that g-NSGA-II did not converge because some objective values of the obtained solutions are more than 1.0. Fig. 15(d) shows the solutions obtained by MOEA/D-a approximating to a small region close to the reference point but the diversity of the obtained solution is not good. Thus, we can see from Table 5, the HV-UM value of MOEA/D-a is smaller than that of MOEA/D-c and IMOEA/D-PRE. Fig. 15(c), (e), (f) presents good diversity and convergence of the obtained solution of IMOEA/D-PRE, MOEA/D-b, MOEA/D-c respectively, so that their HV-UM values in Table 5 are also better than others. In Fig. 16(a), the solutions obtained by g-NSGA-II do not converge into the PF since some objective values are more than 1.0. From Fig. 16(b), although the diversity of the obtained solutions is good, there are still some solutions which do not converge into the region of interest because the $\sum_{i=1}^m f_i^2$ value of the obtained solutions is 1.06433 according to Table 6. Fig. 16(c) and (d) shows that most of the solutions obtained by IMOEA/D-PRE and MOEA/D-a converge into a small region close to the reference point with bad diversity. Fig. 16(e) and (f) presents the solutions obtained by MOEA/D-b and MOEA/D-c having good convergence and diversity. Thus, their HV-UM values and $\sum_{i=1}^m f_i^2$ values also outperform that of others, which can be seen from Table 7.

Overall, on dealing with many-objective problems, MOEA/D-b and MOEA/D-c have better convergence. With the increase of the number of objectives, the aggregation based algorithms especially MOEA/D-b and MOEA/D-c have more advantages to deal with many-objective problems than the Pareto-based approaches.

6. Conclusion

This paper analyzed how to incorporate the preference information with MOEA/D, and proposed three reference points based interactive approaches named MOEA/D-a, MOEA/D-b and MOEA/D-c. The experiments have demonstrated that the proposed approaches have ability to satisfy the DM to find the ROIs interactively. Besides, the approaches could handle the MOPs with many objectives and fit the model with multiple preference information.

During the process of interaction, the DM could specify multiple preference information (like different reference points) to explore his/her interesting ROIs, or to learn some information about the problems. Then, in the following interaction stages, DM could modify the preference information to guide the optimization process to acquire more specific ROIs or other interesting ROIs. One thing should be emphasized that in response to the preference information, the key point in the model is to adjust the weight vectors so as to renew the preference regions.

On the other hand, the proposed algorithms have the ability of providing feedbacks and correcting error decisions to some extent. In other words, the DM could search for his/her interesting solutions or ROIs by means of adjusting the locations of reference points or ranges of ROIs. According to the result of experiments, the proposed approaches can successfully converge into different regions in response to the specified reference points.

However, during the interactive process, there are different sorts of preference information provided by the DM. So, how to express his/her preference information accurately in the system remains to be addressed, thus it would be our future work.

Acknowledgments

This work was supported by the research projects: the National Natural Science Foundation of China under Grant Nos. 61379062, 61403326 and 61502408, the Natural Science Foundation of Hunan Province under Grant No. 14JJ2072.

Appendix A. Supplementary data

Supplementary data associated with this article can be found, in the online version, at <http://dx.doi.org/10.1016/j.asoc.2016.09.032>.

References

- [1] S.F. Adra, I. Griffin, P.J. Fleming, A comparative study of progressive preference articulation techniques for multiobjective optimization, in: Proceedings of the 4th International Conference on Evolutionary Multi-criterion Optimization (EMO'07), 2007, pp. 908–921.
- [2] Q. Zhang, H. Li, MOEA/D: a multiobjective evolutionary algorithm based on decomposition, *IEEE Trans. Evol. Comput.* 11 (6) (2007) 712–731.
- [3] K. Miettinen, Nonlinear Multiobjective Optimization, vol. 12, Springer Science & Business Media, 2012.
- [4] K. Deb, Multi-Objective Optimization Using Evolutionary Algorithms, vol. 16, John Wiley & Sons, 2001.
- [5] C.A.C. Coello, G.B. Lamont, Applications of Multi-Objective Evolutionary Algorithms, vol. 1, World Scientific, 2004.
- [6] J.T. Scruggs, I.L. Cassidy, S. Behrens, Multi-objective optimal control of vibratory energy harvesting systems, *J. Intell. Mater. Syst. Struct.* (2012), <http://dx.doi.org/10.1177/1045389X12443015>.
- [7] D. Corne, C. Dhaenens, L. Jourdan, Synergies between operations research and data mining: the emerging use of multi-objective approaches, *Eur. J. Oper. Res.* 221 (3) (2012) 469–479.
- [8] F. Ahmed, K. Deb, Multi-objective optimal path planning using elitist non-dominated sorting genetic algorithms, *Soft Comput.* 17 (7) (2013) 1283–1299.
- [9] H.M. Fard, R. Prodan, J.J.D. Barrionuevo, T. Fahringer, A multi-objective approach for workflow scheduling in heterogeneous environments, in: Proceedings of the 2012 12th IEEE/ACM International Symposium on Cluster, Cloud and Grid Computing (CCGRID 2012), IEEE Computer Society, 2012, pp. 300–309.
- [10] M. Farina, P. Amato, On the optimal solution definition for many-criteria optimization problems, in: Proceedings of the NAFIPS-FLINT International Conference, 2002, pp. 233–238.
- [11] H. Sato, H. Aguirre, H. E, K. Tanaka, Controlling dominance area of solutions and its impact on the performance of MOEAs, in: Evolutionary Multi-Criterion Optimization, Springer, Berlin Heidelberg, 2007, pp. 5–20.
- [12] M. Laumanns, L. Thiele, K. Deb, E. Zitzler, Combining convergence and diversity in evolutionary multiobjective optimization, *Evol. Comput.* 10 (3) (2002) 263–282.
- [13] K. Deb, M. Mohan, S. Mishra, Evaluating the ϵ -domination based multi-objective evolutionary algorithm for a quick computation of Pareto-optimal solutions, *Evol. Comput.* 13 (4) (2005) 501–525.
- [14] M. Koppen, R. Vicente-Garcia, A fuzzy scheme for the ranking of multivariate data and its application, in: IEEE Annual Meeting of the Fuzzy Information, 2004. Processing NAFIPS'04, IEEE, vol. 1, 2004, pp. 140–145.
- [15] M. Koppen, R. Vicente-Garcia, B. Nickolay, Fuzzy-Pareto-dominance and its application in evolutionary multi-objective optimization, in: Evolutionary Multi-Criterion Optimization, Springer, Berlin Heidelberg, 2005, pp. 399–412.
- [16] E. Zitzler, S. Künzli, Indicator-based selection in multiobjective search, in: Parallel Problem Solving from Nature-PPSN VIII, Springer, Berlin Heidelberg, 2004, pp. 832–842.
- [17] N. Beume, B. Naujoks, M. Emmerich, SMS-EMOA: multiobjective selection based on dominated hypervolume, *Eur. J. Oper. Res.* 181 (3) (2007) 1653–1669.
- [18] J. Bader, E. Zitzler, HypE: an algorithm for fast hypervolume-based many-objective optimization, *Evol. Comput.* 19 (1) (2011) 45–76.
- [19] E.J. Hughes, Multiple single objective Pareto sampling, in: The 2003 Congress on Evolutionary Computation, 2003. CEC'03. IEEE, 2003, pp. 2678–2684.
- [20] K. Deb, H. Jain, An evolutionary many-objective optimization algorithm using reference-point-based nondominated sorting approach. Part I: Solving problems with box constraints, *IEEE Trans. Evol. Comput.* 18 (4) (2014) 577–601.
- [21] P.J. Bentley, J.P. Wakefield, Soft Computing in Engineering Design and Manufacturing, vol. 5, Springer, London, 1998, pp. 231–240.
- [22] S.F. Adra, P.J. Fleming, A diversity management operator for evolutionary many-objective optimisation, in: Evolutionary Multi-Criterion Optimization, Springer, Berlin Heidelberg, 2009, pp. 81–94.
- [23] M. Li, S. Yang, X. Liu, Shift-based density estimation for Pareto-based algorithms in many-objective optimization, *IEEE Trans. Evol. Comput.* 18 (3) (2014) 348–365.
- [24] K. Deb, S. Chaudhuri, K. Miettinen, Estimating Nadir Objective Vector Quickly Using Evolutionary Approaches. Technical Report, 2005.
- [25] H. Ishibuchi, N. Tsukamoto, Y. Nojima, Evolutionary many-objective optimization: a short review, in: IEEE Congress on Evolutionary Computation, Citeseer, 2008, pp. 2419–2426.
- [26] J. Branke, T. Kaußler, H. Schmeck, Guidance in evolutionary multi-objective optimization, *Adv. Eng. Softw.* 32 (6) (2001) 499–507.
- [27] J. Branke, K. Deb, Integrating user preferences into evolutionary multi-objective optimization, in: Knowledge Incorporation in Evolutionary Computation, Springer, 2005, pp. 461–477.

- [28] K. Deb, J. Sundar, N. Udaya Bhaskara Rao, S. Chaudhuri, Reference point based multi-objective optimization using evolutionary algorithms, *Int. J. Comput. Intell. Res.* 2 (3) (2006) 273–286.
- [29] K. Deb, A. Kumar, Interactive evolutionary multi-objective optimization and decision-making using reference direction method, in: Proceedings of the 9th Annual Conference on Genetic and Evolutionary Computation, ACM, 2007, pp. 781–788.
- [30] L. Thiele, K. Miettinen, P.J. Korhonen, J. Molina, A Preference-based Interactive Evolutionary Algorithm for Multiobjective Optimization, 2007.
- [31] J. Molina, L.V. Santana, A.G. Hernández-Díaz, C.A.C. Coello, R. Caballero, g-dominance: reference point based dominance for multiobjective metaheuristics, *Eur. J. Oper. Res.* 197 (2) (2009) 685–692.
- [32] L. Ben Said, S. Bechikh, K. Ghédira, The r-dominance: a new dominance relation for interactive evolutionary multicriteria decision making, *IEEE Trans. Evol. Comput.* 14 (5) (2010) 801–818.
- [33] M. Gong, F. Liu, W. Zhang, L. Jiao, Q. Zhang, Interactive MOEA/D for multi-objective decision making, in: Proceedings of the 13th Annual Conference on Genetic and Evolutionary Computation, ACM, 2011, pp. 721–728.
- [34] A. Mohammadi, M.N. Omidvar, X. Li, Reference point based multi-objective optimization through decomposition, in: 2012 IEEE Congress on Evolutionary Computation (CEC), IEEE, 2012, pp. 1–8.
- [35] A. Jaszkiewicz, R. Słowiński, The 'light beam search' approach—an overview of methodology applications, *Eur. J. Oper. Res.* 113 (2) (1999) 300–314.
- [36] G. Yu, J. Zheng, R. Shen, M. Li, Decomposing the user-preference in multiobjective optimization, *Soft Comput.* (2015) 1–17.
- [37] K. Deb, A. Kumar, Light beam search based multi-objective optimization using evolutionary algorithms, in: 2007 IEEE Congress on Evolutionary Computation (CEC), IEEE, 2007, pp. 2125–2132.
- [38] A.P. Wierzbicki, The use of reference objectives in multiobjective optimization, in: *Multiple Criteria Decision Making Theory and Application*, Springer, 1980, pp. 468–486.
- [39] A.P. Wierzbicki, On the completeness and constructiveness of parametric characterizations to vector optimization problems, *Oper. Res. Spektrum* 8 (2) (1986) 73–87.
- [40] E. Zitzler, K. Deb, L. Thiele, Comparison of multiobjective evolutionary algorithms: empirical results, *Evol. Comput.* 8 (2) (2000) 173–195.
- [41] K. Deb, Multi-objective genetic algorithms: problem difficulties and construction of test problems, *Evol. Comput.* 7 (3) (1999) 205–230.
- [42] D.A. Van Veldhuizen, G.B. Lamont, Evolutionary computation and convergence to a Pareto front, in: Proc. of the Late Breaking Papers at the Genetic Programming Conference, Madison, USA, 1998, pp. 221–228.
- [43] U.K. Wickramasinghe, R. Carrese, X. Li, Designing airfoils using a reference point based evolutionary many-objective particle swarm optimization algorithm, in: IEEE Congress on Evolutionary Computation, 2010, pp. 1–8.
- [44] A.C. Tamhane, Multiple comparisons in model I one-way ANOVA with unequal variances, *Commun. Stat.* 6 (1) (1977) 15–32.